Sustainable re-utilization of waste materials as adsorbents for water treatment

Arnur Omirzakova, Bachelor of Technics and Technology in Chemical Technology of Organic Substances

Submitted in fulfilment of the requirements
for the degree of Master of Science
in Chemical & Materials Engineering

School of Engineering and Digital Sciences
Department of Chemical and Materials Engineering
Nazarbayev University

53 Kabanbay Batyr Avenue,
Nur-Sultan, Kazakhstan, 010000

Supervisor: Stavros Poulopoulos
Co-supervisor: Boris Golman

March 2024

DECLARATION

"I at this moment declare that this manuscript, entitled" "*Sustainable re-utilisation of waste materials as adsorbents for water treatment"*, "is the result of my work except for quotations and citations which have been duly acknowledged."

"I also declare that, to the best of my knowledge and belief, it has not been previously or concurrently submitted, in whole or in part, for any other degree or diploma at Nazarbayev University or any other national or international institution".

Name: Arnur Omirzakova

Date: 15.03.2024

Table of Contents

Abstract

Organic compounds present in polluted wastewater exhibit stability during treatment. Methylene blue, an organic pollutant known for its hazardous oxidative properties, is of particular concern as it is commonly found in the effluent from the textile industry, and its presence in the environment threatens the biosphere. Given the stability of methylene blue dye, sorption via biochar materials emerges as a viable pathway for remediation. Biochar, derived from waste materials such as straw flax and sewage sludge through pyrolysis, is an effective medium. This approach addresses waste management concerns and aligns with the principles of circular economy and environmentally friendly practices. The scope of this work is to study the adsorption properties of biochar from sewage sludge or straw flax in removing methylene blue from water. The working concentration of methylene blue (MB) in water was 20 ppm. Biochar was characterised by various techniques such as Scanning Electron Microscopy, Thermogravimetric Analysis, Fourier Transform Infrared Spectroscopy, and X-ray Diffraction. The biochar efficiency as an adsorbent was proved by the MB removal of 77.33% achieved after 30 min for 220 mg of straw flax-derived biochar with particle size in the 100-400 μm range. Using the sewage sludge-derived biochar (220 mg, 100 μm < d < 400 μm), an MB removal of 30.86% was achieved after 30 min. The straw flax biochar (100 μm < d < 400 μm) showed the lowest thermal tolerance, as 65.71% of it retained its weight at 800 ^{o}C in the N_2 environment. Biochar with particle size distribution ranging in 100-400 μm was more effective than particle sizes in 400-800 μm. The maximum adsorption efficiency observed was 84.37%, and it was achieved by 220 mg of the straw flax biochar with particle size in the range of 100-400 μm after 2 hours. The significance of this investigation lies in its innovative approach to repurposing waste materials generated from pyrolysis for the treatment of water contaminated with the organic dye methylene blue, aligning with the principles of the circular economy.

Acknowledgements

I express my gratitude to professors for their excellent advice and mentoring, which allowed me to implement the given research work in the field of environmental engineering related to water treatment by adsorbents, which were waste materials. I am grateful to Professor Stavros Poulopoulos for providing the necessary equipment and the material base.

List of Abbreviations and Symbols

BET	Brunauer–Emmett–Teller
BPA	Bisphenol A
CH	Coffee Husk
FTIR	Fourier-Transform Infrared Spectroscopy
HTC	Hydrothermal Carbonization
LCA	Life Cycle Assessment
MB	Methylene Blue
nZVI	Nano Zero Valent Iron
PKS	Palm Kernel Shells
PSD	Particle Size Distribution
RH	Rice Husk
SDG	Sustainable Development Goals
SEM	Scanning Electron Microscope
TEM	Transmission Electron Microscope
TGA	Thermal Gravimetric Analysis
UN	United Nations
UV	Ultraviolet
XRD	X-ray Diffraction

List of Figures

List of Tables

Chapter 1. Introduction

Biomass is a renewable, available, and abundant source of Energy. Biomass waste utilisation is valuable given global warming concerns, the need for alternative energy sources, and the circular economy principles. Biomass species utilisation as renewable fuels such as bio-oil and pyrolytic gas has been accelerated by scientists interested in alternative energy sources. (Jiang et. al., 2019)

According to a report by the UN, biomass contributes to 10% of renewable energy consumption through technology and is a share of global energy consumption (United Nations, 2021). Biomass is commonly subjected to pyrolysis. Pyrolysis techniques produced several products, such as pyrolytic gases, bio-oil, tar, and biochar-originated carbonaceous materials. Tar and biochar are considered as pyrolytic intermediates, usually wastes. (Song et. al., 2020). The utilisation of pyrolytic intermediate products is of high significance in the context of the circular economy.

Biochar, which is the product of Hydrothermal Carbonization conversion of biomass, can be functionalised in four main directions: soil remediation, pollution control, energy storage, and catalysis. Biochar's physical properties and surface characteristics are satisfactory for soil remediation. The biochar can be a catalyst by features of surface and structural characteristics. The structural characteristics of biochar are important for Energy. In addition, the biochar's structural and surface characteristics allow it to be employed for pollutant control goals. (Zheng et. al., 2023)

Water is an essential source of life and Energy in the biosphere and for habitats. Considering the vital importance of water in the environment, the purity of water from pollutants is a significant factor for the well-being of nature. Nowadays, water is contaminated with several pollutants from different sources and nature. Consequently, it needs to be treated with various steps and approaches. Well-known harmful pollutants are nitroaromatic compounds, chlorinated compounds, heavy metals, anthropogenic chemicals, and dyes. Among the most toxic contaminants, cationic dye natured methylene blue is a non-biodegradable pollutant. (Abdelfatah et. al., 2021)

The water treatment from methylene blue employs a biochar material. For instance, sewage sludge-originated biochar can be used as an adsorbent for methylene blue removal. The discharge of sewage sludge increases with the time spent accumulating during the sewage treatment. Sewage sludge refers to coproducts in the sewage treatment, and it is counted as a waste material. The sewage sludge is a carbonaceous material which can serve as an adsorbent of an adsorbate. Adsorption is a common technique in water remediation. Consequently, sewage sludge-based biochar is applied to remove methylene blue from polluted water. (Yin et. al., 2022)

The sewage sludge-based biochar can be received from the pyrolysis of the solid residue after the hydrothermal liquefaction during the biocrude production as a coproduct. The municipal sewage sludge is separated from the aqueous phase and the biocrude phase. The biocrude has aliphatic compounds and olefins. The sewage sludge biochar differs by the presence of inorganic elements presence in the composition. After the Soxhlet extraction of the biocrude from the solid residue, the sewage sludge biochar will be available for further modifications and use. (Lauro et. al., 2024)

Following the sewage sludge discharge from the sewage treatment plant and its accumulation can be proposed as a solution for the water treatment plant satisfying the circular economy and waste management. Considering the carbonaceous nature of the sewage sludge-based biochar after the pyrolysis, the specified biochar was applied to the methylene blue removal in this study to evaluate the adsorption characteristics of the sewage sludge biochar. In addition, the straw flax biochar was studied as an adsorbent during the removal of methylene blue from the aquatic environment. The straw flax biochar was selected for this study as it was generated too from the pyrolysis process, and it was counted as a waste material. The straw flax biochar is a carbonaceous material with good adsorption properties for the hydrophobic pollutants in the water.

The thesis consists of (1) an introduction, (2) a literature review on methylene blue removal by biochars, (3) a methodology describing the synthesis of biochars for further applications, (4) results and discussion, and (5) a conclusion suggesting further improvements. In this work, the adsorption characteristics of the sewage sludge biochar and the straw flax biochar were described and evaluated, and the solution was evaluated for 20 ppm methylene blue.

Chapter 2. Literature Review

2.1 Zero Waste as an Approach for Circular Economy

The pollutant control through the functionalisation of biochar produced from agricultural residues was conducted for cadmium remediation by sorption techniques where biochar's raw materials were quinoa, coffee husk (CH), oil palm kernel shells (PKS), blend (PKS+C). The effective excess loading was satisfied with quinoa, which was about 60 mg Cd/ g biochar. At the same time, specified biochar was tested in methylene blue adsorption experiments. The raw biochar's surface area of quinoa was approximately 450 m^2/g, which was defined during the measurements of the methylene blue experiment. (Lopez et. al., 2020)

The geometric and volumetric properties of biomaterials were expanded. Often, it was considered a bulk volume. At the same time, the bulk volume was subdivided into envelope volume, apparently volume, and absolute volume. Consequently, the density term was extended to bulk density and envelope density. (Yan et al., 2020). The density was related to the porosity characterisation in terms of surface properties analysis. The particle size, combined with density and porosity characteristics, would describe the surface properties following the determination of the biochar's application area.

Rice husk's-based biochar's application for mercury removal was implemented through Hg^{2+} adsorption onto the biochar. Japan supported the recycling of rice husk as an adsorption material for water treatment directions. The rice husk accumulation in one year was 2,000,000 tons. The modified rice husk's-based biochar showed a higher Hg^{2+} adsorption capacity, 330 mg/g, than the raw rice husk's-based biochar, 223-253 mg/g. The Kinetics of raw and chlorine-modified rice husk's-based biochar were different. RH biochar corresponded to the pseudo-first-order kinetic model, while chlorine-modified RH was satisfied to the pseudo-second-order kinetic model. (Mochizuki et. al., 2020)

Biochar technology was satisfied with the principles of the hydrogen H_2 society, which supported the achievement of the UN's SDGs. The main products of pyrolysis were employed as an alternative source of Energy, while biochar was applied to water treatment systems for water-splitting approaches. Camellia japonica flowers originated from biochar, which was used to capture carbon. In addition, Camellia japonica flowers originated from biochar, which was employed as an electrode material for water-splitting voltage in electrochemical directions. (Igalavithana et. al., 2022)

Phosphorus pollution in the agricultural sector could be solved through water treatment by employing Ca-doped biochar. The main idea was Ca^{2+} coprecipitation with P atoms, and P adsorption was observed, too. The kinetic aspect corresponded to a pseudo-second-order kinetic

model. The pyrolysis thermal conditions of biomass affected their adsorption capacities. The 673.15 K produced adsorbent that had 53.22 mg/g, while 1073.15 K was satisfied with 17.77 mg/g. (Zhang et al., 2021). Sewage sludge-originated biochar was subjected to upgrading. The waste upgrading led to the plants' fertilisation directions. Undoped biochar could be a treating material as it had higher extractability than Ca, Mg, Al, and Fe-doped biochar. At the same time, it served for carbon sequestration purposes. (Buss et. al., 2020)

2.2 Clean water and sanitation by Sustainable developments goals of the UN

Water purification techniques are related to various approaches. Adsorption technology can be applied to purify water, including urban water and municipal wastewater. Sustainable Assessment is significant in reaching the 6th goal of the UN's SDG. Local and global LCA impact rankings on environmental conditions are mutually connected. Water contamination significantly affected the life quality of civilians. Adsorption technology corresponds to the removal of heavy metals, methylene blue, nitrate, ammonium, phosphate, and crystal violet. Each adsorbate was satisfied with the bioadsorbent, in other words, biochar (activated carbons). The stable organic pollutants in water were methylene blue, toluidine blue, rhodamine B, gaseous formaldehyde, amoxicillin, methyl orange, and malachite green. (Tran et. al., 2023). The target organic pollutant was methylene blue.

Water treatment and energy storage were combined through sodium alginate recycling techniques. Sodium alginate polymerisation was alternatively substituted with synthetic, non-biodegradable, and non-renewable materials. Sodium alginate polymer chains were applied to the water treatment of heavy metals removal such as Cu, Co, Pb, Cr, and Cd. In addition, it was applicable for methylene blue and methyl orange removals. (Wang et. al., 2023)

Oil-water separation by sustainable adsorbents was reached through the development of super-hydrophobic SiO_2 nanoparticle-fabricated spent coffee grounds (SSD-SCGs). The developed SSD-SCGs allowed us to achieve the 6th goal of the SDGs of the UN. The viscous crude oil removal efficiency of SSD-SCGs was about 98.5-99.7%. It was capable of destroying stable oil-water-oil emulsions. (Shi et. al., 2023)

2.3 Organic compounds contamination in water treatment systems

Organic pollutants could vary depending on their contamination source in the water treatment area. Consequently, organic contaminants in water could originate from industry, households, agronomy, and other possible areas. From medical sources, wastes could originate from organic contaminants such as antibiotics of different applications and complex compositions.

Currently, antibiotic contamination counts as a significant environmental concern. For this goal, different removal active substances are used. With the chemical approach of water treatment, a broad application of metal-organic frameworks originating from the organometallic approach, along with the application of transition metals, is noticed. The transition metals are part of d-block elements. Zinc is one of the d-block elements and could serve as a MOF component for antibiotics removals such as tetracycline, nitrofurans, and chloramphenicols. (Gai et al., 2020). The main problems there were antibiotic resistance to the treatment and water contamination.

From household sources, organic compounds might be personal care products such as sunscreen components. For instance, active components of a sunscreen such as octinoxate, homosalate, and avobenzene serve as UV adsorbents; however, they are non-biodegradable compounds, which means water contamination with organic compounds. (Chou et al., 2024). In the sewage treatment plant, organic compounds could be treated in contaminated water. The main technique is adsorption, which is a physical approach to the removal of contaminants. Hydrophobic pharmaceuticals in water can be removed through the application of activated carbon materials. The main advantage of activated carbon is the non-generation of any hazardous coproducts during the water treatment. As a source of activated carbon, it may serve as biochar material. Biochar materials are advanced by their porous structure, increased surface areas, and hydrophobic nature. (Chakraborty et al., 2023)

Biochars are applicable for dye removal from wastewater. One of the dyes that are used as a water contaminant is known as methylene blue. Methylene blue might have originated in wastewater from the industry along with methyl red, congo red, crystal violet, methyl orange, and rhodamine B. They are water-soluble as their nature is organic salt. Then, it causes problems in water treatment, such as photosynthetic activity, and harms the aquatic biosphere. Following that, a solution for water treatment is needed. Activated biochars may adsorb organic dyes such as methylene blue. Biochars demonstrated their enhanced activity in removing organic contaminants in water treatment. The pH medium is an important factor during the sorption experiment. For methylene blue, pH=8 is satisfied as an optimal value. One of the advantages of biochar's application during the removal of organic contaminants is its reusability and long-term sustainability. The reusability is available through the regeneration with the reflux in ethanol for 30 min following separation and vacuum drying. The reactivation of biochar is reached at 105 ^{o}C. In the optimised case, methylene blue of 20 mg/L could be removed for 94.51% in 15 min. The methylene blue adsorption is characterised by a pseudo-second-order model. (Vashisht et al., 2024). Methylene blue is known as a reactive oxygen species generator due to photosensitiser in

the presence of UV light. The reactive oxygen species are hazardous for the biodiversity in the aquatic medium as they support oxidative damage to cellular components.

Metal oxide/biochar material is applicable in water treatment. Depending on its removal mechanism, it could be used in adsorption or in catalysis directions. Metal oxide/biochar hybrids are synthesised a little bit differently than pure biochar. There were two ways of preparing biomass: pre-treatment and post-treatment. The synthesis method might be varied depending on their further use goals. Dewatered sewage sludge-based biochar hybrids with TiO_2, Fe, and Fe_3C are applicable for methylene blue removal by adsorption with photodegradation methods, and the removal efficiency is 89.2% at 800 ^oC pyrolysis temperature. The reed straw-based biochar hybrids with Zinc and TiO_2 are applicable for adsorption with the photocatalysis degradation method, and the removal efficiency is 80.8% at 500 ^oC pyrolysis temperature. (Weidner et. al., 2022). Metal impregnation increases the specific surface area and adsorption efficiency in the direction of chemical modification of biochar's surfaces.

Removal mechanisms might be various for adsorption experiments. For instance, electron donor-acceptor interactions, precipitation, hydrophobic attractions, pore filling, electrostatic interactions, and ion exchange. The biochar application minimises adverse effects and enhances the removal of contaminants for a circular, sustainable economy. In the dye remediation directions, electrostatic attraction, pore-filling, complexation, and ion exchange are usually satisfied. In addition to these, hydrophobic effects are also met. Especially for methylene blue adsorption experiments, it is satisfied by an electrostatic attraction removal mechanism. For methylene blue removal enhancement, the temperature might be increased before 50 ^oC as it enhances an extraction rate through the adsorption. (Joshi et. al., 2023)

Methylene blue can be extracted from wastewater through the employment of waste material such as biochar, which accumulates in different directions. For instance, peanut shells can be pyrolysed under oxygen-limited conditions at 500 ^oC followed by biochar generation. The ZnO-modified peanut shells-based biochar is capable of removing the methylene blue from the water in 5 min with the adsorption capacity of 645 mg/g, and in 2 hours, it becomes 700 mg/g for 50 ppm methylene blue solution. (Luyen et. al., 2023)

Carbon-rich solid materials such as biochar from waste materials in the methylene blue removal show various adsorption efficiencies. For instance, straw-based biochar materials behave differently from peanut shells-based biochar. The straw biochar has shown the maximum adsorption capacity of 4.75 mg/g at 20 ppm methylene blue. For the chemical adsorption of methylene blue, the optimal temperature for the straw biochar is 35 ^oC at pH=7.00. (Zheng et. al., 2023)

The flax biochar application in the methylene blue removal from the polluted water can be achieved with the adsorption capacity of 18 mg/g at 20 ppm methylene blue solution in ambient conditions. By increasing the thermal parameter, the adsorption capacity of the flax biochar is increased to 45 mg/g at 20 ppm methylene blue. The acidic modification of the flax biochar is affected positively, and the adsorption capacity becomes 75 mg/g at 20 ppm methylene blue. (Zeghioud et. al., 2022)

The novelty of the research

This research work will provide water treatment from methylene blue by the application of an unmodified waste-derived biochar as an adsorbent in the aquatic medium. It could be used in wastewater treatment plants for methylene removal. Furthermore, biochar-based waste materials support circular economy approaches as they serve as an adsorbent of organic pollutants in water treatment.

Research questions:

1. How does the waste-derived biochar of the sewage sludge nature remove the methylene blue from the aqueous medium at ambient conditions and in the light absence?
2. What is the adsorption behaviour of the straw flax-originated biochar in 20 min for the methylene blue removal?

The goal is to evaluate waste-derived biochar's application in methylene blue removal from the aquatic medium.

Objectives:

1. The particle size distribution of waste-derived biochars;
2. Methylene blue adsorption by the sewage sludge biochar;
3. Methylene blue removal by the straw flax biochar;
4. The comparison of two waste-derived biochar's adsorbent behaviours.

Chapter 3. Methodology

3.1 Biochar's synthesis

The raw material for biochar preparations was flax straw biomass, which was accumulated in Northern Kazakhstan. The dried flax straw biomass was subjected to dispersion with grinding through the employment of a rotatory cutting mill of the model RM 120 of the brand Vibrotechnik, which accompanied the decrease in particle size and optimisation. Thermal treatment of dried flax straw biomass through the employment of an oxygen-free conditioned horizontal tube furnace. The setup was drawn in Figure 1. The thermal treatment unit consisted of a manometer, tubular furnace, nitrogen tank, quartz tube and thermostat, control panel, filter and gas analyser, flowmeter, and impingers. The quartz tube's thermal condition was monitored by applying a thermocouple of type K, which was embedded into the system for the furnace temperature control and conditioned through the thermostat. Oxygen-free conditions were achieved through the employment of nitrogen gas, such as an inlet gas, which was managed through a calibrated flowmeter of the brand Dywer. The isopropanol solution of 99.7% was employed for two-stage condensation in impingers, which collected the waste material – tar. The second product of the pyrolysis, together with pyrolytic gas, was biochar. Biochar was received from the quartz tube in the appearance of black powder. (Mukhambet et. al., 2022).

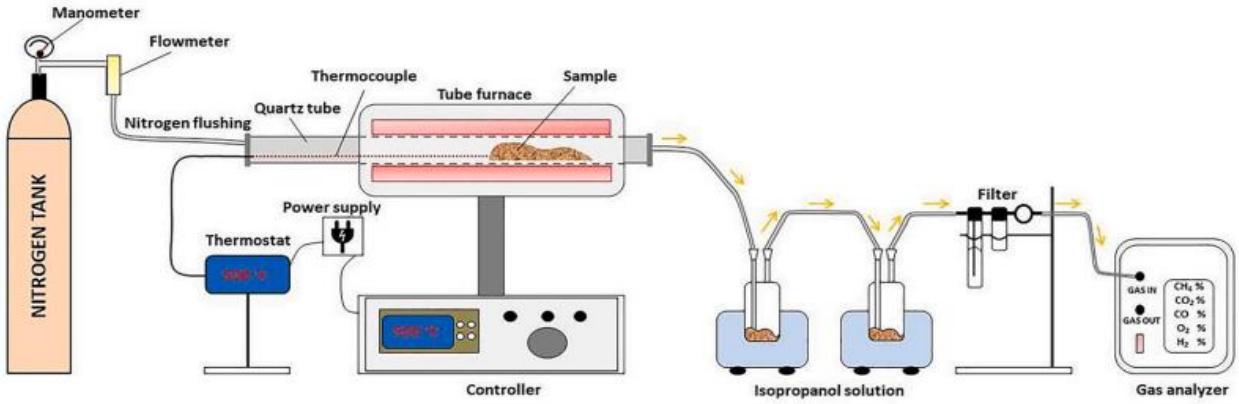

Figure 1. The technical scheme of flax straw biomass pyrolysis. Reproduced from (Mukhambet et al., 2022). Copyright 2022 Elsevier. Reprinted with permission.

The pyrolysis conditions were set up as furnace temperature was 773.15 K, and the heating rate was 303.15 K/s. Into the fixed bed reactor was introduced 20 g (±0.1) flax straw biomass. Pyrolysis target product for this research – biochar's yield was defined by the equation (1):

$$C_{CY,\%} = \frac{W_{CY}}{SDW} \times 100, \quad (1)$$

where were W_{CY} – mass of biochar, g; SDW – mass of dried flax straw biomass, g; $C_{CY,\%}$ – biochar's yield, %.

The comparative biochar was received from the sewage through the same pyrolysis technique; however, thermal treatment conditions were various. The thermal condition in the furnace was 773.15 K, and the heating rate was managed as 0.159 K/s. The nitrogen gas flow rate was about 0.06 m^3/s. The pressure was set as 1 MPa. The continuance of the pyrolysis was 20 min. The input of the sewage for the biochar preparation was 10 g (±0.1). The yield of the biochar was figured out by equation (1), where SDW is the mass of sewage.

3.2 Biochar's particle size distribution

Granular biochar was subjected to the sieve analysis to determine the particle size distribution's content ranging in size starting from d < 100 μm ending with 1000 μm < d. In the case of laboratory conditions, a system of mechanical sifting with a set of metallic wire sieves with square hole side sizes d < 100 μm, 100 μm < d < 400 μm, 400 μm < d < 800 μm, 800 μm < d < 1000 μm, 1000 μm < d was employed. The mechanical sieving system was serviced without an integrated vibration drive; consequently, the sieving procedure was carried out in a manner that corresponded to the human hand vibration mode. The sieving analysis results would be satisfied with the Gaussian distribution depending on the biochar's nature. The sieving metallic wire sieves parameters were given in Table 1 (911 Metallurgist, 2023).

Table 1. The sieve's geometrical parameters.

The wire diameter, mm	Width of opening, μm
0.054-0.073	88
0.063-0.087	105
0.079-0.103	125
0.20-0.29	350
0.23-0.33	420
0.26-0.37	500
0.33-0.48	710
0.38-0.55	840
0.43-0.62	1000

The sieve analysis setup consisted of a pallet, sieves, a covering cap, and stable fixation of sieves.

3.3 Methylene Blue removal by biochar's

The removal of methylene blue from the contaminated water was carried out only for kinetic analysis, which meant time-dependent adsorption of methylene blue onto biochar at room temperature and atmospheric pressure conditions in the absence of the light source. Methylene

blue dye (ACROS Organics, CAS 61-73-4, pure 99.9%) was considered like an organic pollutant which served as an adsorbate. Methylene Blue would be harmful if swallowed. At the same time, methylene blue would be the primary health concern due to its ability to decrease the oxygen carried in the blood. Methylene blue spoils negatively charged cell components, which are a kind of nucleic acid. Methylene blue is applied in biology and medicine to see the sample under the optical microscope. For instance, during the cystoscopy, methylene blue might be visible in the urinary tract. Cancer research might identify bladder cancer cells. The chemical structure of the methylene blue affected its thermal stability, and the heating of the methylene blue would lead to the decomposition and the emission of toxic fumes. The adsorbate characteristics were conditioned with their own high molar extinction coefficient. The light source absence during the kinetic study was related to the property of methylene blue to absorb the visible light. Consequently, a UV-Vis spectrophotometer can monitor the methylene blue's adsorption onto the biochar.

The experiment was conducted with a continuance of 2 hours in total. The working concentration of methylene blue was 20 mg/L (20 ppm). The preparation of methylene blue required high accuracy due to its dye properties, which might paint anything. Consequently, after the measurement of its weight, it was shown to dissolve by water and block its loss during the transfer from the balance to the volumetric flask. To investigate the kinetics of methylene blue adsorption onto biochar, it was monitored the UV-Vis adsorption of several different methylene blue – biochar contact times every 15 minutes sampling before the 2 hours of the experiment. Each of the experiments was completed twice for the data reproducibility and at least the duplicity.

The experimental setup consisted of the shaker, beaker-like reactors, and fume hood (light source blocking). The experimental procedure had several steps such as the methylene blue stock solution's preparation, its Quantification before the kinetic study, to measure the weight of biochar, ready methylene blue containing reactors transfer under the fume hood, biochar's addition into the methylene blue solution. After the addition of biochar into the solution, time should be measured for the sampling every 15 minutes.

The kinetic study of methylene blue adsorption onto biochar was considered for managing the biochar's concentration to 20 ppm of methylene blue. For instance, 10, 40, 70, and 100 mg of biochar were used for 25 mL of 20 ppm methylene blue solution where the shaking mode was 400 rpm. The comprehensive kinetic study of the adsorption of methylene blue on biochar consisted of the implementation of experiments for all possible particle size distribution ranges. The common techniques of the whole kinetic study were presented in Table 2 and Table 3. Table 2 showed straw flax biochar, which was similar to sewage biochar samples in Table 3. The table was provided for clarity on the experimental procedure and to follow it. The main idea was to variate

the biochar mass to significantly differentiate for the observation of the biochar's concentration to the methylene blue adsorption rate on the surface of biochar and to identify the adsorption characteristics for the specified particle size distribution.

Table 2. The comprehensive kinetic study of methylene blue adsorption onto flax straw biochar.

#	Biochar mass	Particle size distribution	
	mg	100 μm < d < 400 μm	400 μm < d < 800 μm
1	2	3	4
2	10	2	2
3	40	2	2
4	70	2	2
5	100	2	2
6	160	2	2
7	220	2	2
Total tests - 24		12	12

Table 3. The comprehensive kinetic study of methylene blue adsorption onto sewage biochar.

#	Biochar mass	Particle size distribution	
	mg	100 μm < d < 400 μm	400 μm < d < 800 μm
1	2	3	4
2	100	2	2
3	160	2	2
4	220	2	2
Total tests - 12		6	6

Tables demonstrated the biochar's mass variation, which could be increased by the needs.

3.4 Analytical procedures

3.4.1 Characterisation of synthesised material

Biochar samples were characterised through the application of modern instrumental tools for the study of their physicochemical properties. The materials characterisation methodology was based on non-destructive techniques such as FTIR, SEM, XRD, etc. However, the destructive technical approach was employed too. For instance, the thermal characteristics of biochar samples were studied using the TGA method.

The field emission scanning electron microscope analysis was implemented on SEM Crossbeam 540 of the manufacturer Carl Zeiss. The SEM analysis was completed according to the sample preparation technique without any coatings to reduce a surface's charge, and copper-based adhesive tape was used. The copper-based adhesive tape was chosen considering the nature of biochar samples as they consisted of carbon compounds. The operational conditions of the equipment were given in Table 4. The SEM Crossbeam 540 magnification was varied for samples to achieve better resolution of SEM pictures, as shown in Table 5. The morphology of the adsorbent's surface was pictured at several magnifications for better comparative analysis. FE-SEM equipment's technical scheme was given in Figure 2. The specified equipment was examined in the adsorbent surface morphology description and the geometrical parameters identification step. It was significant when it was related to the heterogeneous phase of the treating compound's interaction with the adsorbent's surface as a contact area, and time would be affected by the efficiency of the adsorbent.

Table 4. SEM Crossbeam 540 working conditions for biochar morphology.

#	Name of the parameter for SEM imaging	Satisfying value for the parameter
1	2	3
2	Signal A	Inlens
3	EHT	5kV
4	I probe	70pA
5	Scan Speed	3
6	Column Mode	High Resolution

Table 5. SEM Crossbeam 540 magnification variation for biochar morphologies better resolution.

#	The sieve's-based size distribution	flax straw biochar	sewage biochar
1	2	3	4
2	100 μm < d < 400 μm	200, 350, 500, 1k, 5k, 10k, 20k	200, 500, 1k, 5k, 10k, 20k
3	400 μm < d < 800 μm	200, 350, 500, 1k, 5k, 10k, 20k	200, 500, 1k, 5k, 10k

The FE-SEM operational technical scheme contained several parts for the operational state.

Electrons are released out of a field emission origin, and then in a high electrical field gradient, was accelerated. Inside the high vacuum column, these qualified primary electrons are oriented and deflected through electronic lenses to generate a narrow scan beam that attacks the sample. Therefore, secondary electrons are emanated from a spot on the object. The angle and

secondary electrons' velocity touches the surface structure of the sample. A detector captures the secondary electrons and accordingly releases an electronic signal. The considering signal is enhanced and turned into a video scan image that can be visible on a monitor or a digital image that can be preserved and transformed further. (Radboud University Nijmegen, 2023)

Another non-destructive physicochemical method of analysis was X-ray diffraction, which was employed to examine the phase of substances, especially the presence of crystal lattice in the composition of the substance. The XRD analysis was capable of identifying the nature of the crystal lattice and the empirical formula of the crystal through the software Match from the brand Crystal Impact. (Crystal Impact, 2023).

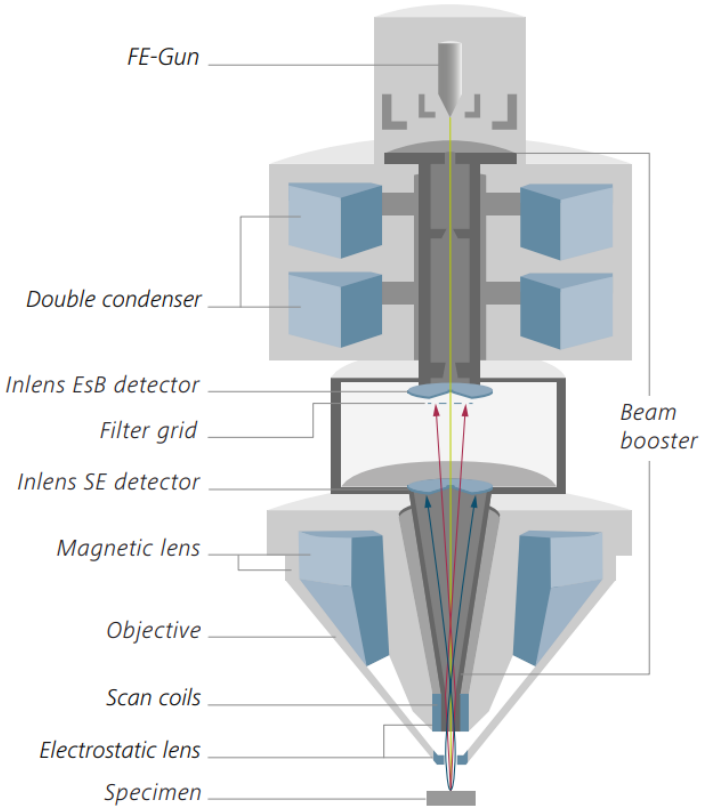

Figure 2. FE-SEM technical scheme (ZEISS, 2023).

The powder diffraction XRD analysis was carried out using the X-ray Diffraction (XRD) System – SmartLab of the manufacturer Rigaku. In situ, powder diffraction XRD spectrum analyses were conducted in the selected region of XRD patterns of biochar samples with the 2θ range of 20−80°. The technical parameter: Ni-K β absorber (1.5444[OBJ]) filtered Cu-K α-radiation (1.5406[OBJ]) in a standard Bragg−Brentano geometry. The generator voltage was 50 ,kV and the

tube current was 40 mA. The step size was 0.01. The equipment required a powder sample satisfying all samples were dispersed before powders during the sample preparation as all biochar samples were solid particles. (Nav*Ȧ*a et. al., 2020) The equipment required a powder sample satisfying all samples were dispersed before powders during the sample preparation as all biochar samples were solid particles. (Navarathna et. al., 2020)-radiation (1.5406*Ȧ*) in a standard Bragg−Brentano geometry. The generator voltage was 50 kV and the tube current was 40 mA. The step size was 0.01. The equipment required a powder sample satisfying all samples were dispersed before powders during the sample preparation as all biochar samples were solid particles. (Navarathna et. al., 2020) The equipment required a powder sample satisfying all samples were dispersed before powders during the sample preparation as all biochar samples were solid particles. (Navarathna et. al., 2020)

Fourier-Transform Infrared Spectroscopy analysis was conducted on the equipment Nicolet iS10 FT-IR Spectrometer of Thermo Fisher Scientific. The specified analysis was conducted with 34 repetitions in the range of 400-4000 cm^{-1} of wavelength. The goal of the analysis was the identification of biochar samples' functional groups of organic nature-based fragments. (Bibi et. al., 2023). The functional group identification was relevant, considering that a water pollutant was methylene blue, which was an organic compound, too. In the given region were fundamental vibrational transitions that were in the mid-IR wavelength range, in other words, the region of electromagnetic waves.

Thermal Gravimetric Analysis was implemented for the biochar thermal stability test and to evaluate the pyrolysis behaviour of biomass components in the thermal range of 30-800 ^oC and under the secondary vacuum as N_2 atmosphere where the heating rate was 10 ^oC/min on the Simultaneous Thermal Analyser (STA) 6000 of the manufacturer Perkin Elmer. It is practicable to evaluate the Energy of activation (E_a) of biochar as a function of the conversion degree with no precondition requirement for the reaction mechanism of decomposition. (Osman et. al., 2020)

3.4.2 Quantification of methylene blue

Methylene blue Quantification was conducted on the UV-Vis spectrophotometer in the wavelength range of 600 nm^{-1} – 700 nm^{-1} where the target measuring peak was satisfied at 664 nm^{-1}. It corresponded to the highest peak for methylene blue species. The working principle of methylene blue quantification was satisfied with the Beer-Lambert-Bouguer law (equation 2) which was expressing the dependence of light absorbance's logarithmic difference (Doble et. al., 2023). The given graph for the calibration was the dependence of the light absorption from the

methylene blue concentration. The ideal calibration curve equation should be *y=ax-b* where R^2=1.00. The line's slope described the methylene blue's extinction coefficient.

$$A = \log_{10}\frac{I_0}{I} = \varepsilon \cdot c \cdot l = -\log_{10}\frac{I}{I_0} = -\log T \quad (2)$$

were, A – absorbance, I_0 – incident light intensity, I – transmitted light intensity, T – transmittance, ε – molar absorptivity coefficient, l – path length through the sample cell, c – methylene blue concentration.

The methylene blue calibration solutions were prepared from the stock solution of 20 ppm 100 mL. The stock solution was diluted for the specific concentrations of 10 mL such as 0, 0.5, 1.0, 2.5, 5.0, 7.5, and 10.0 ppm. The prepared solutions were transferred to the quartz cuvette specific for the UV-Vis spectrophotometer. The UV-Vis spectrophotometer was set up for absorbance measurement instead of transmittance measurement. The scanning speed – was medium, and each point of the scanning – was 2 nm^{-1}. The measuring lines were selected as 625 nm^{-1} and 664 nm^{-1}. The quantified dependence of light absorbance from methylene blue concentrations was transferred to the calibration line for further Quantification of methylene blue concentrations during kinetic studies.

Before the Methylene Blue removal experiments, the UV-Vis spectrometer calibration for MB quantification was at 664nm. The calibration curve was represented in Figure 3. The satisfied data was represented in Table 6. As described in the methodology the calibration was completed before 10 ppm of MB as its detection limit of MB at UV-Vis spectrophotometer.

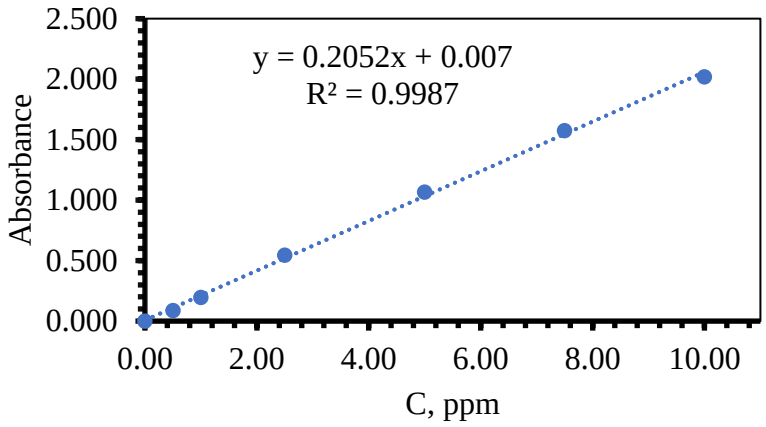

Figure 3. UV-Vis calibration for MB quantification.

The proper UV-Vis calibration for MB quantification was conducted with high accuracy and precision as R^2=99.87% which was acceptable.

Table 6. UV-Vis calibration for MB quantification.

#	C, ppm (MB)	Absorbance at λ=625 nm^{-1}	Absorbance at λ=664 nm^{-1}

1	2	3	4
1	0	0.000	0.001
2	0.5	0.045	0.087
3	1	0.101	0.196
4	2.5	0.292	0.544
5	5	0.593	1.067
6	7.5	0.909	1.573
7	10	1.220	2.018

Methylene blue quantification during kinetic studies of its adsorption onto biochar samples was conducted with the same technique as the calibration step. However, in the case of kinetic studies, it was subjected to define methylene blue concentrations through the light absorbance at spent time of adsorption experiments. This methylene blue quantification allowed us to monitor its removal by biochar in contaminated water. The important notice for methylene blue quantification during kinetic studies was to separate biochar particles before analysis. The methylene blue quantification characteristics were the next three curves such as adsorption percentage by spent time, remaining MB concentration by spent time, and adsorbed MB amount by spent time.

The adsorption percentage was identified by the equation 3. Adsorption capacity was evaluated by equation 4. by the equation 3. Adsorption capacity q_t was evaluated by equation 4.

$$\%A = \frac{(C_0 - C_t)}{C_t} \cdot 100\,, \tag{3.4.2.2}$$

$$q_t = \frac{(C_0 - C_t) \cdot V}{W}, \tag{3.4.2.3}$$

where C_0 – the initial concentration of the MB solution, ppm; C_t – the concentration of the remaining MB in the solution, ppm; V – the volume of the solution, mL;W – the weight of the biochar sample, mg.

Chapter 4. Results and Discussion

4.1 Materials characterisation

Materials characterisation was implemented considering the nature and visible properties of biochar samples. The non-destructive physicochemical analysis method was preferred. Therefore, the morphology of the adsorbent's surface was examined by the field emission scanning electron microscope. For SEM characterisation, two biochar particle distributions were 100 µm < d < 400 µm and 400 µm < d < 800 µm for both samples. The obtained result was demonstrated in Figure 4 with a magnification of 200.

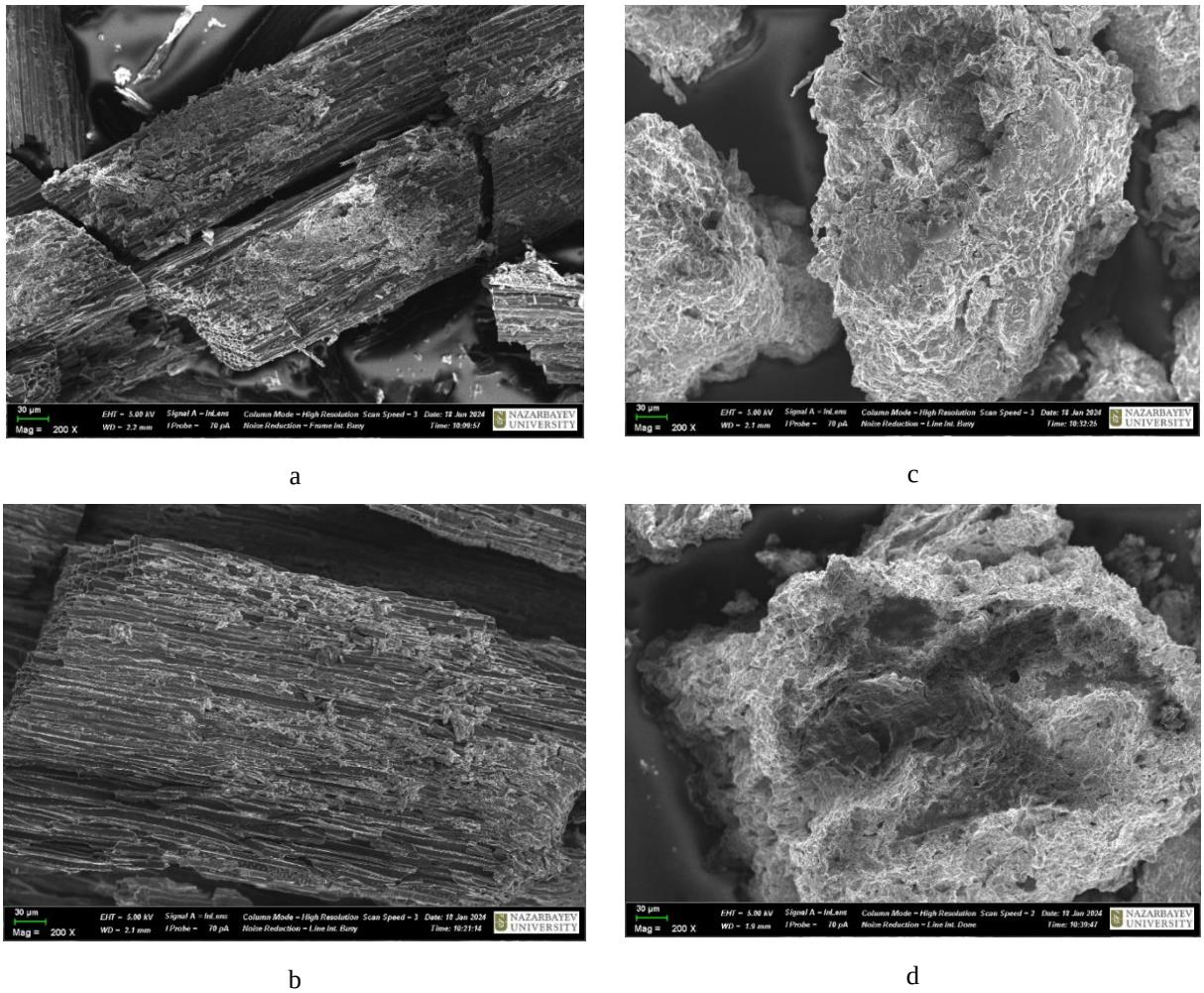

a c

b d

a – 100 µm < d < 400 µm, b – 400 µm < d < 800 µm of the flax straw biochar; c – 100 µm < d < 400 µm, d – 400 µm < d < 800 µm of the sewage biochar

Figure 4. SEM pictures of biochar samples at magnification 200.

SEM pictures demonstrated satisfying morphologies of the adsorbent's surfaces. There were illustrated roughly porous solid amorphous micron particles of different shapes satisfying their nature. In the case of Figures 4.a and b, the nature of raw material for the pyrolysis was affected by the further shape of adsorbent micron particles. Therefore, on specified pictures were noticed

several carbon micro-tubes which were porous and will affect as a physical adsorbent for further application in the water treatment. Figures 4.c and d were demonstrated shapeless at the same time ball-shaped semi-porous amorphous patterns which sometimes were charged by the study area displacement.

The magnification 200 demonstrated the general morphology of biochar samples; however, there were not enough to conclude their morphologies. Therefore, the magnification was increased several times and manifested in Figure 5 with a magnification of 5.00k.

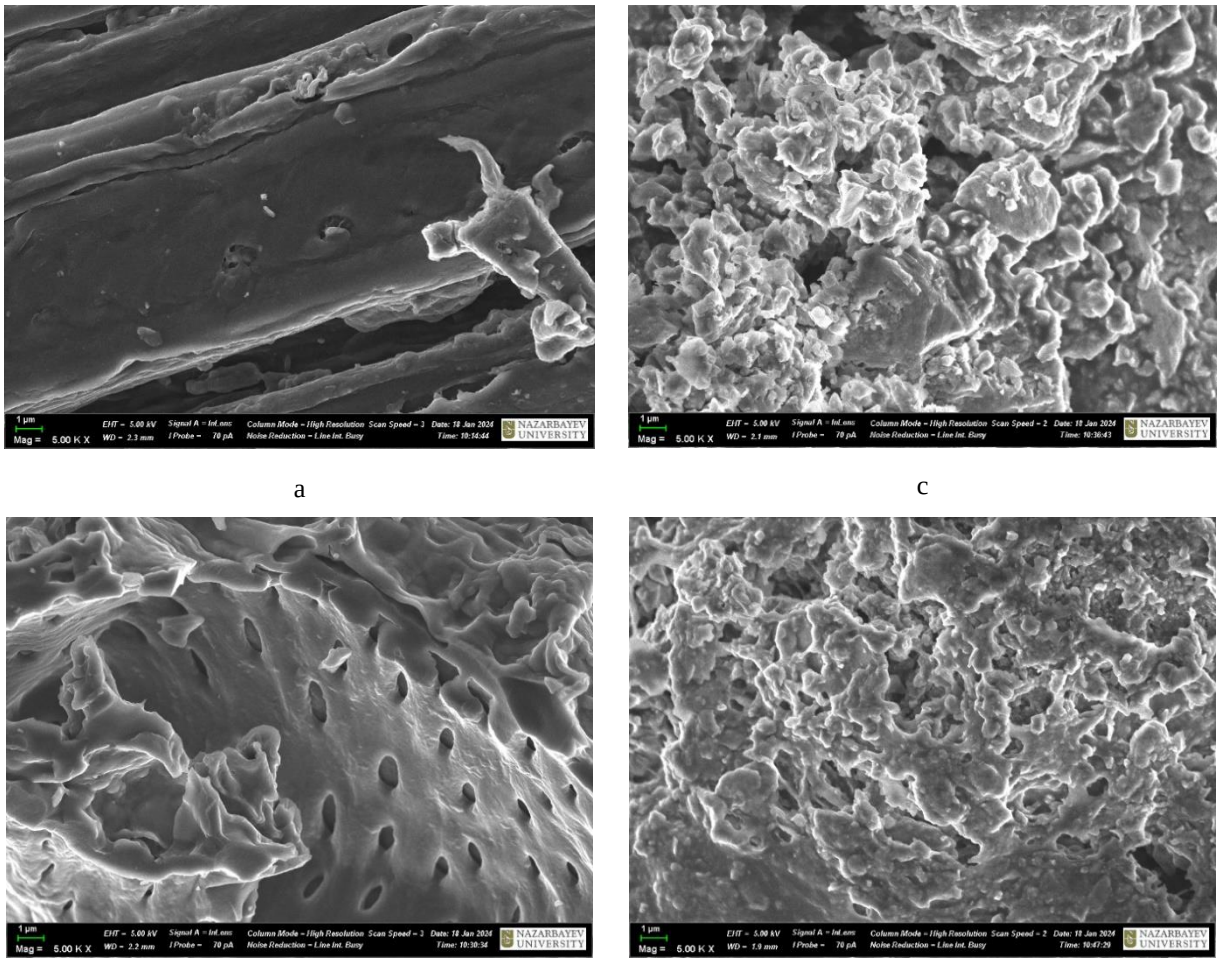

a c

b d

a – 100 µm < d < 400 µm, b – 400 µm < d < 800 µm of the flax straw biochar; c – 100 µm < d < 400 µm, d – 400 µm < d < 800 µm of the sewage biochar

Figure 5. SEM pictures of biochar samples at magnification 5000.

The several times increased magnification gave results on the morphology examination. Structural differences compared to biochar samples were shown. The flax straw biochar samples consisted of macro-pores as in Figure 5.a and b which were noticed without the porosimeter analysis for the BET approach. The flax straw biochar was pure comparatively to the sewage biochar samples as has been noticed in Figures 5.c and d. These figures indicated the presence of

inhomogeneous surfaces with foreign objects that differ in nature from the main mass, which can be concluded that these are pollutants.

On both biochar's different particle distribution ranges were pictured porous surfaces of adsorbents. The last sample was charged during the picturing of SEM results which indicated the presence of a charging substance, which most often has an inorganic nature, as well as a crystal lattice. Consequently, these samples were subjected to XRD analysis to confirm the working condition of the SEM and the validity of the obtained drawings. The particle charges can be seen in Figure 5.d which are particularly displayed as horizontal lines. The subsequent results of the XRD analysis are presented as a graph in Figure 6.

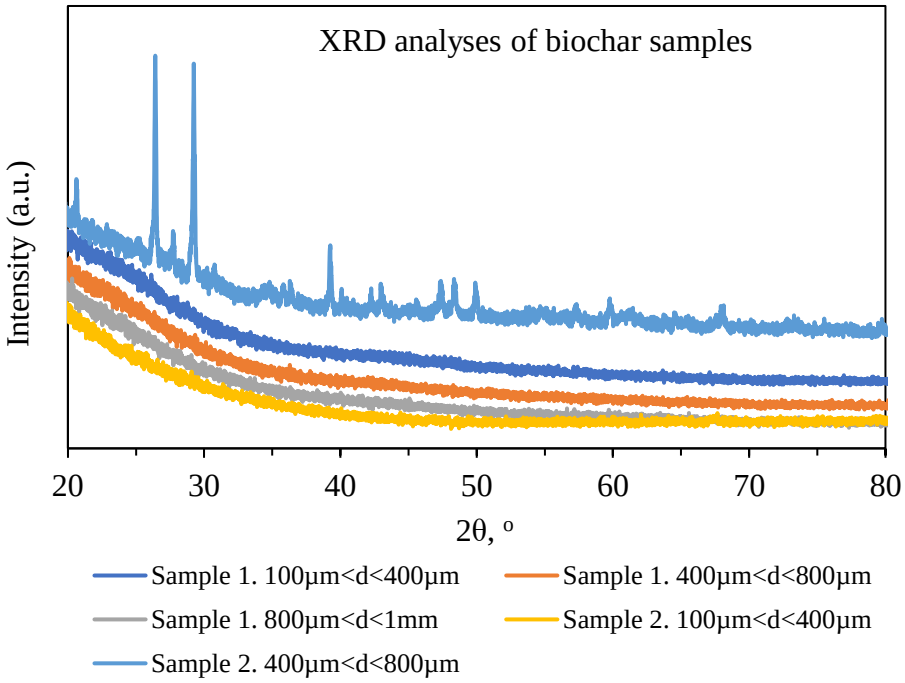

Figure 6. PDXRD analyses of flax straw biochar and sewage biochar samples.

Figure 6 were given powder diffraction XRD analysis results for flax straw biochar (Sample 1) materials and sewage biochar (Sample 2) materials. There were shown curves for three biochar samples' particle distribution ranges as 100 µm < d < 400 µm and 400 µm < d < 800 µm which made up the bulk of biochar samples. In addition, the bigger range 800 µm < d < 1000 µm was examined too for the flax straw biochar.

PDXRD curves of samples were informed about their phases and only one sample had a crystal lattice which was a sewage biochar of 400 µm < d < 800 µm particle size. Therefore, PDXRD analysis approved the SEM picture of the specified sample. From the curves of all other samples, it was concluded as an amorphous phase of substances.

After the approval of the phase of samples the nature of samples was studied through FTIR analysis which allowed for characterisation by the identification of specific bonding then functional groups were discovered. The curve of FTIR analyses was drawn in Figure 7.

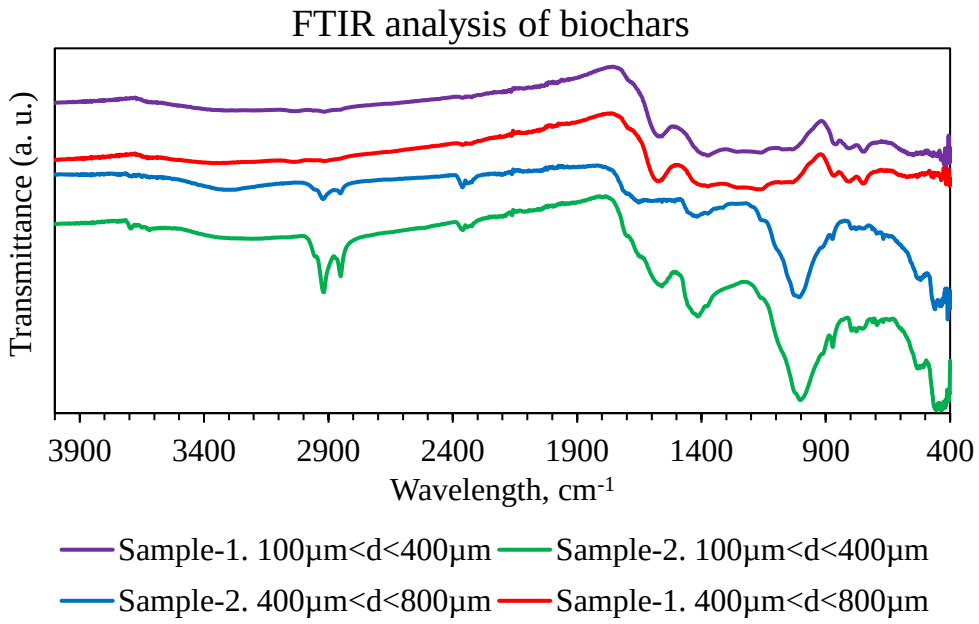

Figure 7. FTIR analyses of biochars.

FTIR analyses significant peaks could be represented in the table as Table 7.

Table 7. Biochars' FTIR analyses significant peaks.

#	Sample-1. The straw flax biochar		Sample-2. The sewage sludge biochar	
	100 µm < d < 400 µm	400 µm < d < 800 µm	100 µm < d < 400 µm	400 µm < d < 800 µm
1	2	3	4	5
1	2916.05	3354.74	2918.96	3322.32
2	1567.98	2152.65	2850.49	2921.45
3	1373.67	1574.51	2359.81	2360.76
4	858.63	1373.42	1558.84	1418.51
5	746.03	1160.65	1413.50	1007.38
6	545.11	866.31	1003.77	518.56
7	470.12	807.52	872.02	460.39
8	453.21	750.74	777.08	436.93
9	437.65	575.44	529.81	417.19
10	425.29	474.94	430.65	
11	417.18	467.03		
12		436.20		

FTIR analyses of biochar samples prove the organic nature through the presence of functional groups. In the sample-1 which was the straw flax biochar, terminal vinyl olefins were detected in fingerprint regions of 1000-900 cm^{-1} (-CH=CH- trans, carbon-hydrogen deformation vibrations), 1630-1690 cm^{-1} (non-conjugated carbon-carbon stretching vibrations), and 3100-3050 cm^{-1} (-CH=CH_2 vinyl, carbon-hydrogen stretching vibrations) in the 100 µm < d < 400 µm which is characteristically for C=C bond in the structure. In the same sample in fingerprint regions of 1420-1460 cm^{-1} (symmetric stretching vibrations), 1540-1580 cm^{-1} (asymmetric stretching vibrations) were satisfied to aliphatic carboxylic acid salts. In sample-1 of 400 µm < d < 800 µm, the composition showed the same functional groups. Only intensities are different. The FTIR analysis does not show any characteristic O-H bond for humidity presence, which means a fully dried substance has an active form. FTIR analyses of sewage sludge biochar showed functional groups such as aliphatic hydrocarbons and aliphatic carboxylic acid salts. Aliphatic carboxylic acid salts were in the range of 1558.84 cm^{-1} (O-C=O asymmetric stretching vibrations). At 2918.96 cm^{-1} is asymmetric C-H stretching, and at 2850.49 cm^{-1} are symmetric C-H stretching vibrations, which are characteristic of aliphatic hydrocarbons. 1413.50 cm^{-1} is satisfied with the O-H bend, which means the moisture presence in the sample by its nature. 1003.37 cm^{-1} is satisfied to -CH_2 stretching vibrations. Both sizes had the same composition.

Thermal gravimetric analyses of biochars were completed to study their degradation behaviours. The observed results were represented in Figure 8.

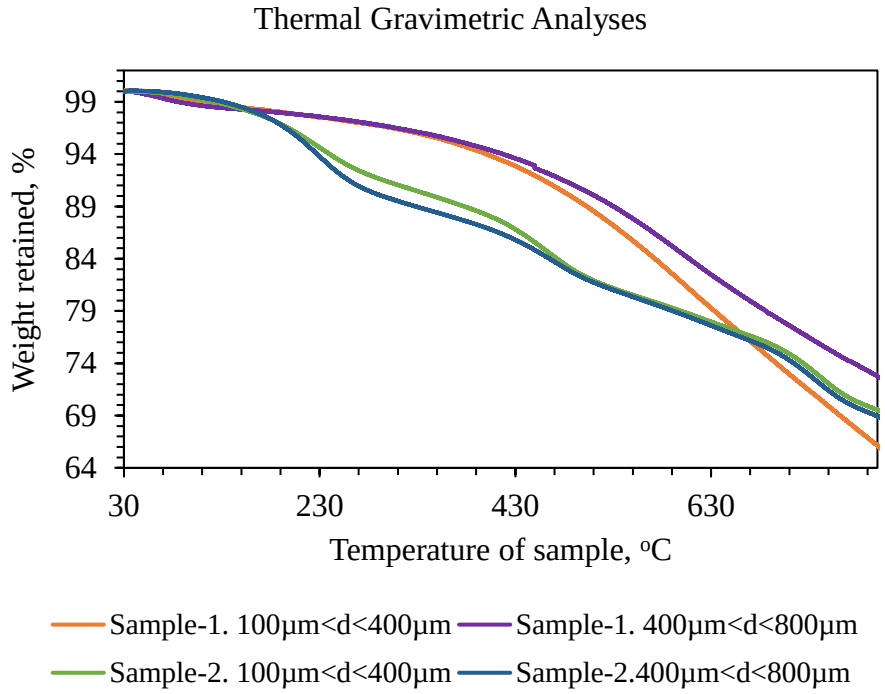

Figure 8. TGA analyses of biochars.

TGA analyses of biochar samples were drawn as thermal stable substances. The pyrolysis temperatures of biochars were the same at 500 ^{o}C. TGA analyses were completed before 800 ^{o}C. The weight retained and the weight loss at those temperatures were represented in Table 8.

Table 8. TGA analyses key points for biochars.

#	Biochar sample	TGA – 500 ^{o}C		TGA – 800 ^{o}C		Total, %
		Weight loss, %	Weight retained, %	Weight loss, %	Weight retained, %	
1	2	3	4	5	6	7
1	Sample-1. 100 μm < d < 400 μm	10.85	89.15	34.29	65.71	100
2	Sample-1. 400 μm < d < 800 μm	9.45	90.55	27.60	72.40	100
3	Sample-2. 100 μm < d < 400 μm	17.65	82.35	30.72	69.28	100
4	Sample-2. 400 μm < d < 800 μm	17.82	82.18	31.32	68.68	100

Thermal stabilities of biochar were stable before the pyrolysis temperature, and after that, they started to lose weight of biochar. The biochar had an organic nature, and any compounds in the composition had their temperature volatility. Following that, after 500 ^{o}C were released CO_2 as some organic compounds were decomposed. In Table 8, their thermal stabilities were clearly shown. Comparatively to other samples, the most stable sample was the straw flax-based biochar of 400 μm < d < 800 μm size range. The most unstable sample was the sewage sludge biochar of 400 μm < d < 800 μm size range at 500 ^{o}C. However, at 800 ^{o}C the most-unstable sample was the straw flax-based biochar. Considering the nature of biochar and its composition, it was demonstrated that particle size was important for the straw flax biochar, while the particle size didn't affect the thermal stability of the sewage sludge biochar. It indicated that the composition of samples could be slightly different for various particle sizes in the structure of the straw flax biochar. In addition, it might affect the adsorption efficiency of the biochar depending on their particle size.

4.2 Biochar's particle distribution

Synthesised biochar was subjected to sieving to separate particles by size distribution. Flax straw biochar and sewage biochar showed the particle size distribution tendency in Figure 9. The histogram presented that the main particle sizes were characteristically in the range of 400 μm < d < 800 μm and 100 μm < d < 400 μm in both cases. The obtained biochar's particle size distribution described that the pyrolysis conditions originated with higher particle size and the preparation of high-quality biochar. Flax straw biomass-originated biochar was subjected to different particle-

sized biochar formations on the specified conditions. The histogram showed all possible particle size ranges starting from d < 100 μm till 1000 μm < d.

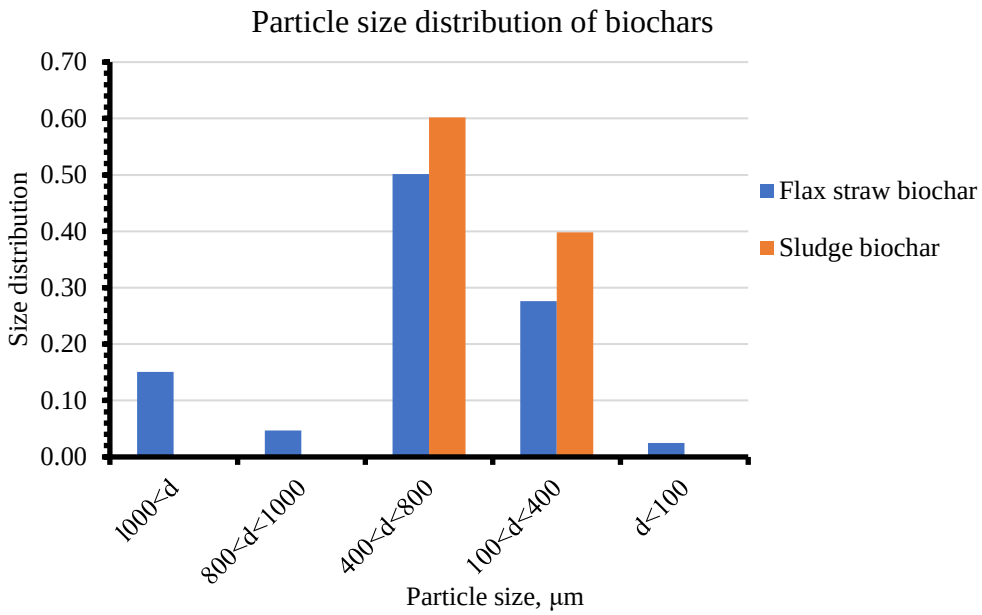

Figure 9. Particle size distribution of synthesised biochar.

Figure 9 manifested various particle size ranges for flax straw biomass-originated biochar. It is conditioned by the nature of the raw material. Consequently, the satisfying particle size distribution corresponded to size ranges, for instance, d < 100 μm – 2.483%, 100 μm < d < 400 μm – 27.605%, 400 μm < d < 800 μm – 50.135%, 800 μm < d < 1000 μm – 4.697%, 1000 μm < d – 15.08%. The less particle size distribution was satisfied to the d < 100 μm range. On the same histogram, the sewage-originated biochar's particle size distribution characteristics were represented, too. The difference in the nature of the raw material was significantly observed. The specified biochar's particle size distribution corresponded only to two size ranges specifically, in 100 μm < d < 400 μm – 39.816%, and in the range of 400 μm < d < 800 μm – 60.184%. In other size ranges, they were not separated biochar particles.

Received biochar yields were calculated for the total mass and the specific particle size distribution range according to the equation (3.1). The specified particle size distribution yields were presented in Figure 10. The total yields of both biochar samples were different according to the nature of employed raw materials which were subjected to the pyrolysis. The total yield for the flax straw biomass-originated biochar was 27.785% while the total yield for the sewage-originated biochar was about 87%. As the histogram presented the biochar yield for d < 100 μm, 800 μm < d < 1000 μm ranges were insignificant for the flax straw biomass originated biochar. The TOP-3 yields for the given biochar were 100 μm < d < 400 μm – 7.67%, 400 μm < d < 800 μm – 13.93%,

1000 µm < d – 4.19%. The presented yields for each particle size distribution were described and the pyrolysis process was not selective for the biochar preparation.

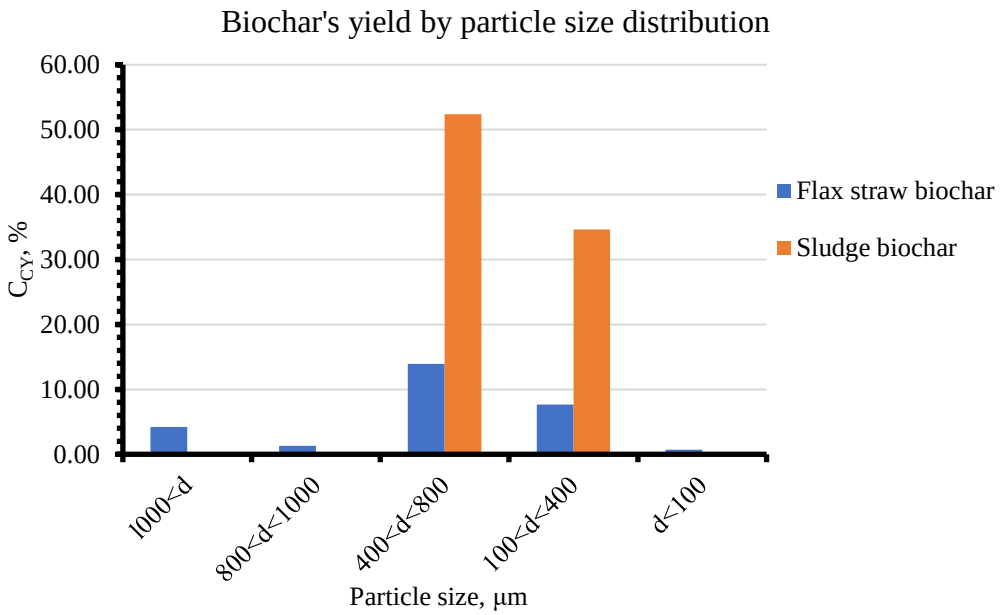

Figure 10. Biochar's yield by particle size distribution.

Visual pictures of the particle size distribution were represented in Figures 11 and 12.

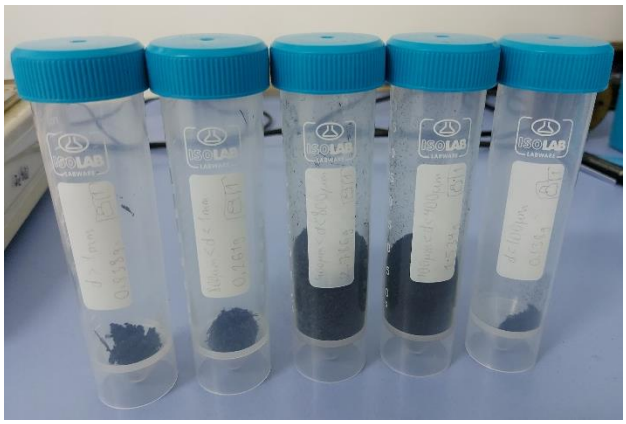

Figure 11. Flax straw biomass originated biochar's particle size distribution.

Sewage-originated biochar's yield was subjected to a separate analysis by the particle size ranges too. Figure 10 demonstrated that 100 µm < d < 400 µm – 34.64% and 400 µm < d < 800 µm – 52.36% which in summary gave 87%. The total yield of the obtained biochar specified that the pyrolysis process was selective to the high-quality biochar preparation compared to the pyrolytic gas synthesis and the waste material – tar formation. The separate particle size range showed the significant values of the yield.

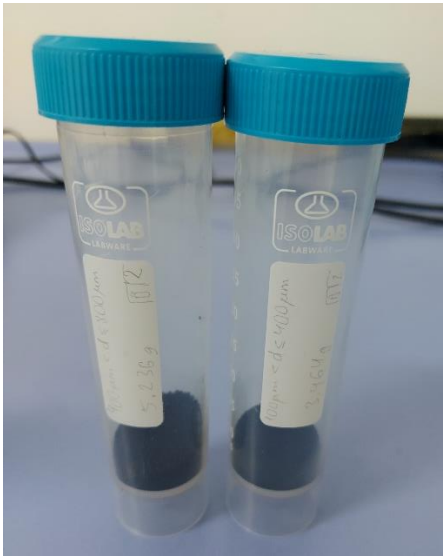

Figure 12. Sewage-originated biochar's particle size distribution.

The high selectivity of the pyrolysis process allowed to employment of biochar as an adsorbent for the water treatment system according to the zero-waste approach and 6th goal of the Sustainable Development Goals of the United Nations (United Nations, 2023). The 6th goal of SDG of UN was named for clean water and sanitation which meant the improvement of water's quality too and could be related to the water treatment.

4.3 Methylene Blue removals in the water treatment characterisation

4.3.1 Methylene Blue removal by the adsorption of sewage sludge biochar

Methylene Blue removal experiments were conducted in the absence of light with various weight loads of active biochar samples of different particle sizes in the aquatic medium. The adsorption study was initiated from the sewage sludge biochar of 10 mg in 20 ppm of methylene blue. The reason for the first choice is explained by its target particle size distribution which meant a much amount of sample comparatively to the straw flax biochar samples. The particle size effect at 10 mg of the sludge biochar was represented in Figure 13. On the graph the adsorption characteristics are not clear; however, it showed 20% adsorption in 15 min and after 30 min it behaved as no further adsorption of MB. The effective contact time by the graph is 15 min which means a fast adsorption of MB. The particle size range 100 µm < d < 400 µm was more effective than 400 µm < d < 800 µm. However, it could not be concluded now. Then it needed to increase the weight load of biochar samples.

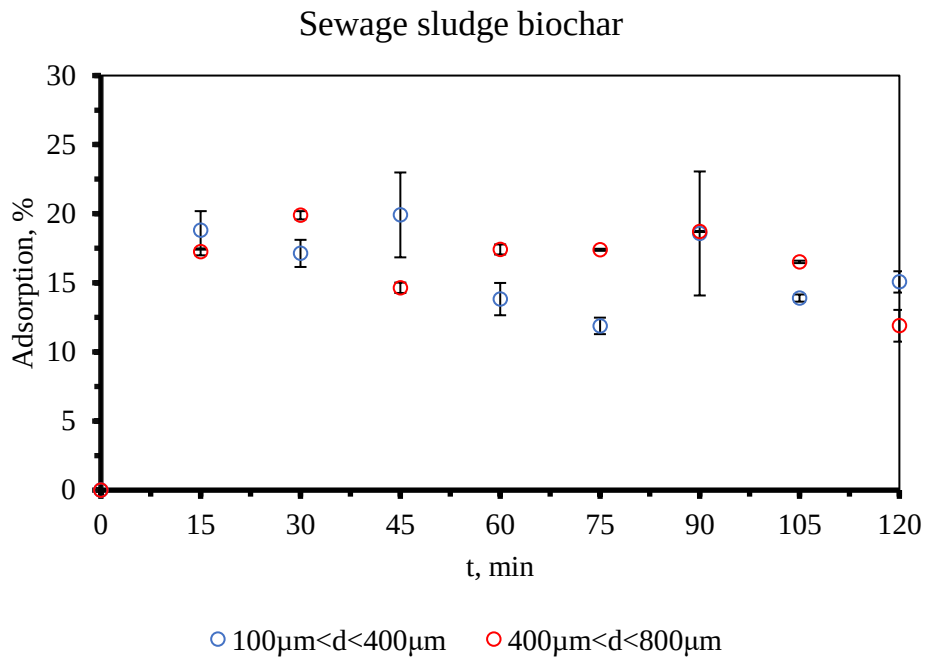

Figure 13. 10 mg weight load for 20 ppm MB removal.

The MB concentration change by time during removal was represented in Figure 14. The initial concentration was 19.6 ppm, and it was reduced to about 15.9 ppm at 15 min. At 30 min the MB was desorbed back from 100 µm < d < 400 µm, and again adsorbed at 45 min. The same behaviour was satisfied to 400 µm < d < 800 µm at different sampling times. The adsorption and desorption were continued before the end of the experiments.

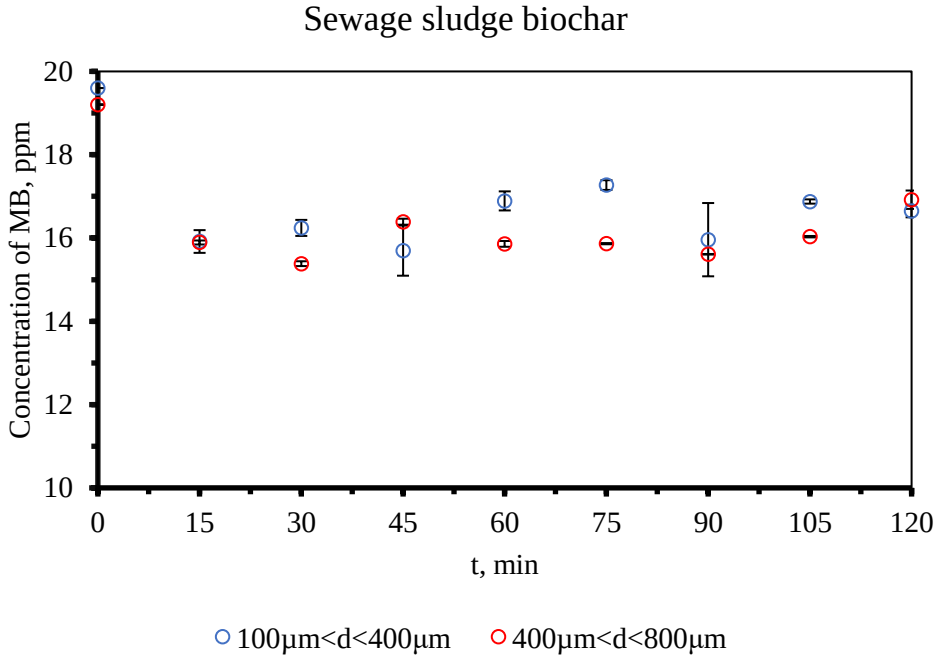

Figure 14. Methylene blue removal at 10 mg of the biochar.

Adsorbed methylene blue q_t by spent time was drawn in Figure 15 in other words it was an adsorption capacity of the biochar —the same behaviour of the graph in Figure 13.

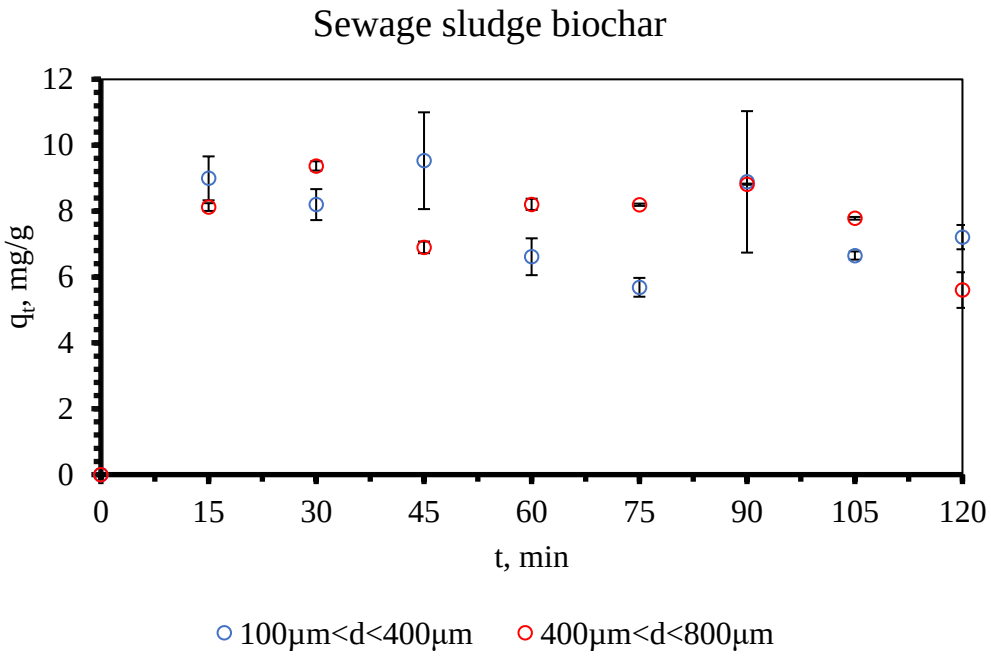

Figure 15. Adsorption capacity of sewage sludge biochar of 10 mg for 20 ppm MB experiment.

The sewage sludge biochar weight load was increased before 40 mg for a 20 ppm MB experiment. The same indicating curves were drawn in Figure 16, Figure 17, and Figure 18.

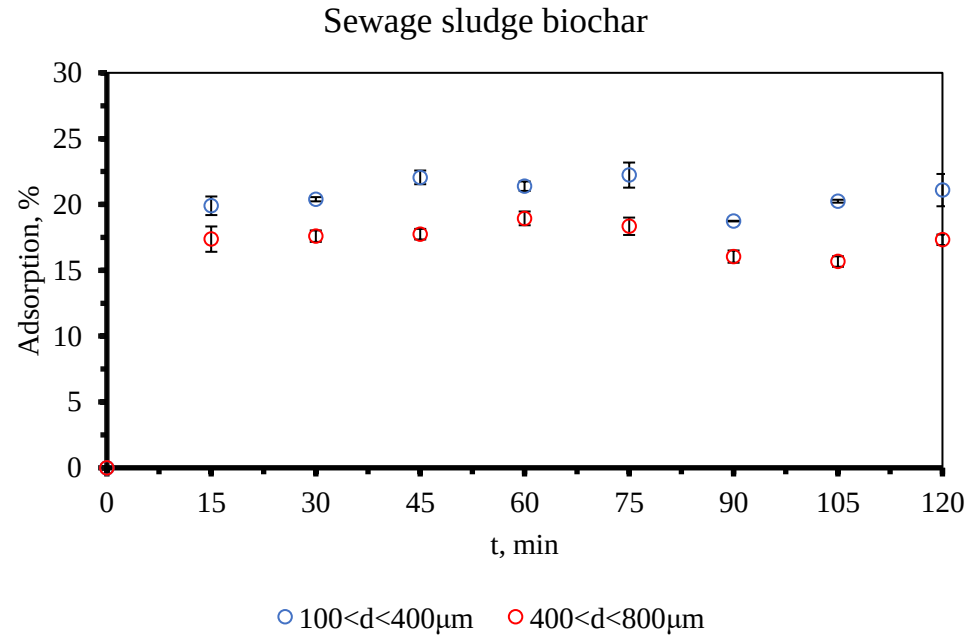

Figure 16. 40mg weight load for 20 ppm MB removal.

Figure 16 showed that MB adsorption was continued before 45 min; however, the fast adsorption was kept at 15 min. On this graph, comparable characteristics were noticed for different particle sizes of biochar samples. The adsorption efficiency of 400 µm < d < 800 µm was significantly lower than for 100 µm < d < 400 µm. In addition, the graph indicated that 100 µm < d < 400 µm adsorbed more comparatively to its last time before 45 min when 400 µm < d < 800 µm had an insignificant difference in adsorption efficiency at the same period. Comparatively to Figure 13 of 10 mg weight load in this case the adsorption took place for 30 min longer and could reach 22.06% of adsorption at 45 min when 18.79% for 15 min of 10 mg of 100 µm < d < 400 µm. At 15 min of 40 mg weight load, the adsorption was 19.92% for 100 µm < d < 400 µm while for 400 µm < d < 800 µm was 17.37%.

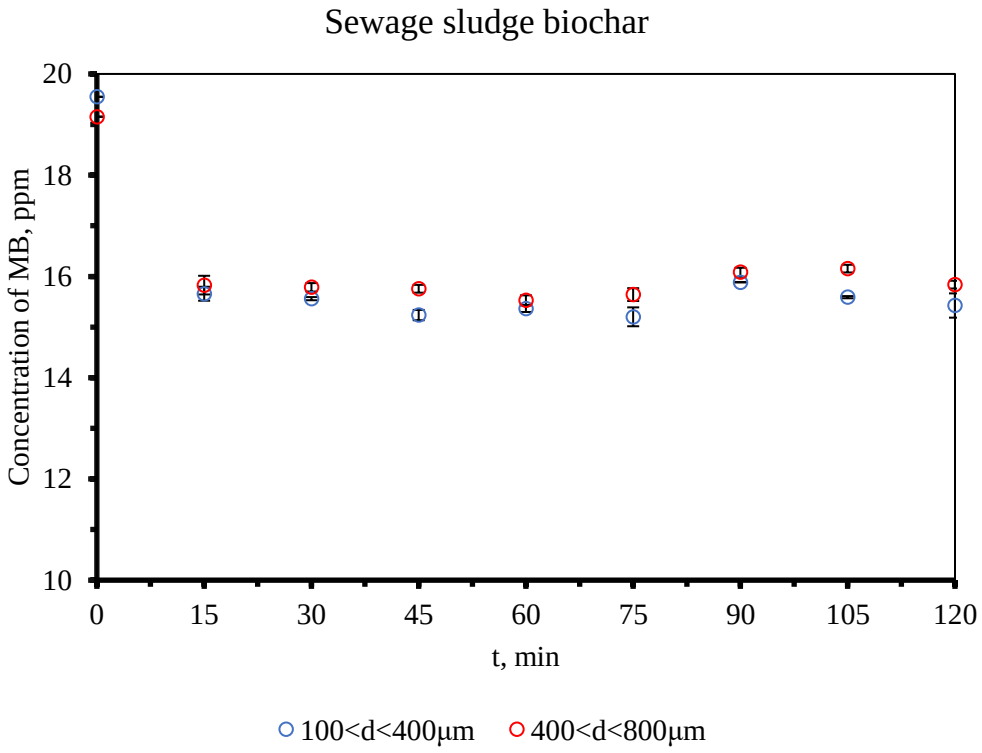

Figure 17. Methylene blue removal at 40 mg of the biochar.

The curve of MB concentration reduction was inverse to the graph of MB adsorption. There were shown that concentration was reduced to 15.24 ppm from 19.55 ppm for 100 µm < d < 400 µm of sewage sludge biochar. Comparatively to Figure 14 on this graph was drawn that desorption of MB has occurred later and with less difference of concentration by last spent time. This graph described the limitation step clearly. However, it did not explain the removal way behaviour.

Followed that the sampling time should be changed to the range of 0 – 15 min. Then, the sampling time was settled as 0, 1, 5, 10, 15 minutes.

The adsorption capacity of sewage sludge biochar was decreased from 40 mg comparatively to 10 mg. In the case of 10 mg, the largest adsorption capacity was 0.0095 at 15 min for 100 µm < d < 400 µm while for 40 mg was 0.003 at 45 min of the same particle size. It was explained by the loading weight of biochar. The adsorption was not grown significantly; however, the weight of biochar was increased significantly.

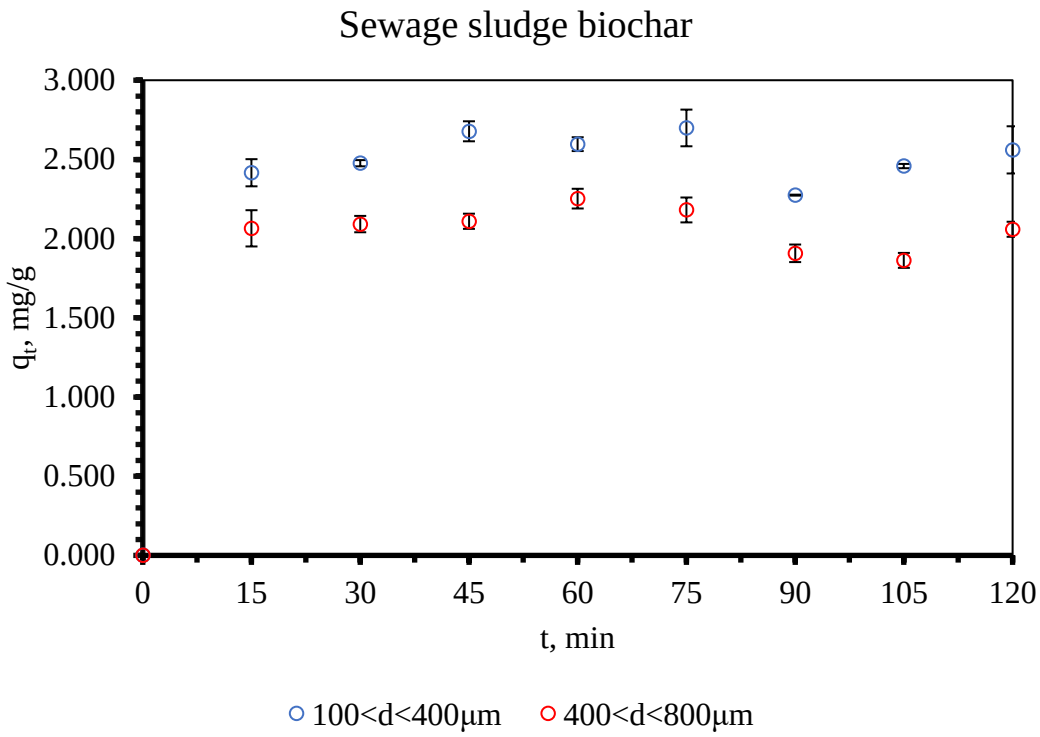

Figure 18. Adsorption capacity of sewage sludge biochar of 40 mg for 20 ppm MB experiment.

Another affecting factor for the adsorption experiment was the volume of MB solution. In the above cases, the volume of MB solution was 25 mL. The comparison was experimented with 3 mg of sewage sludge biochar and 15 mL of MB solution. In the case of 15 mL, it showed more removal efficiency. The observed results were given in Figures 19, 20, 21. There were some interesting outputs. The removal efficiency was 57.74% at 15 min then by spent time it was reduced before 19% for 100 µm < d < 400 µm which meant immediate desorption and it had a low capacity to kept extracted MB from the solution. Figure 20 proved that adsorbed MB species were desorbed again, and it was not applicable for water treatment from MB contaminants. The variation of the volume would not increase the total adsorption efficiency.

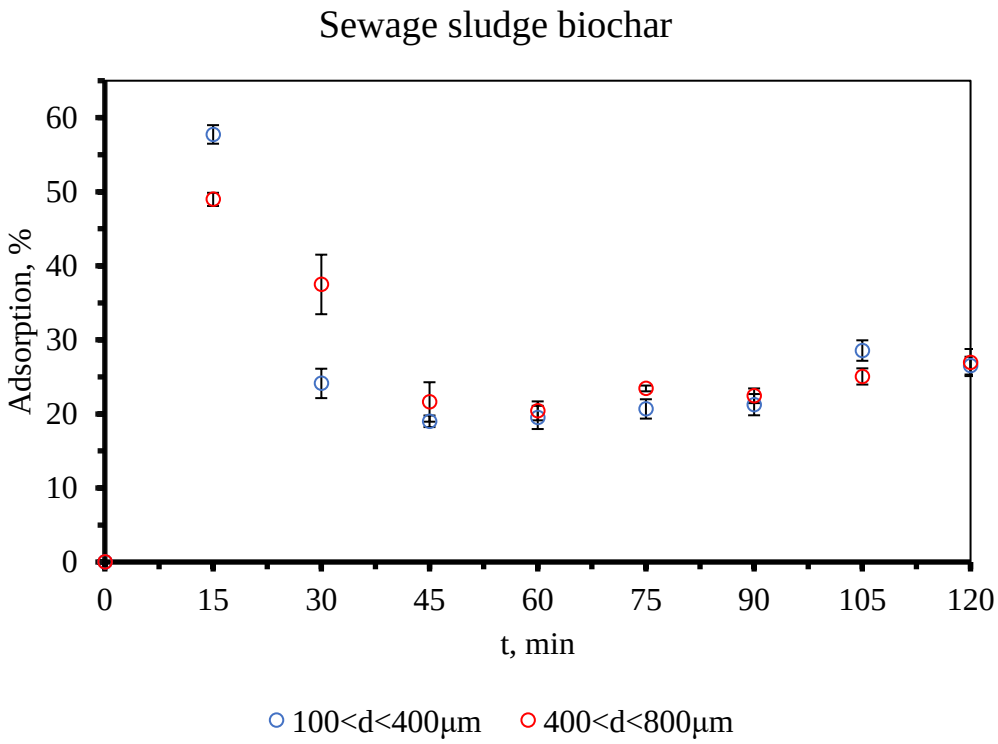

Figure 19. 3 mg weight load for 20 ppm MB removal and 15 mL of MB solution.

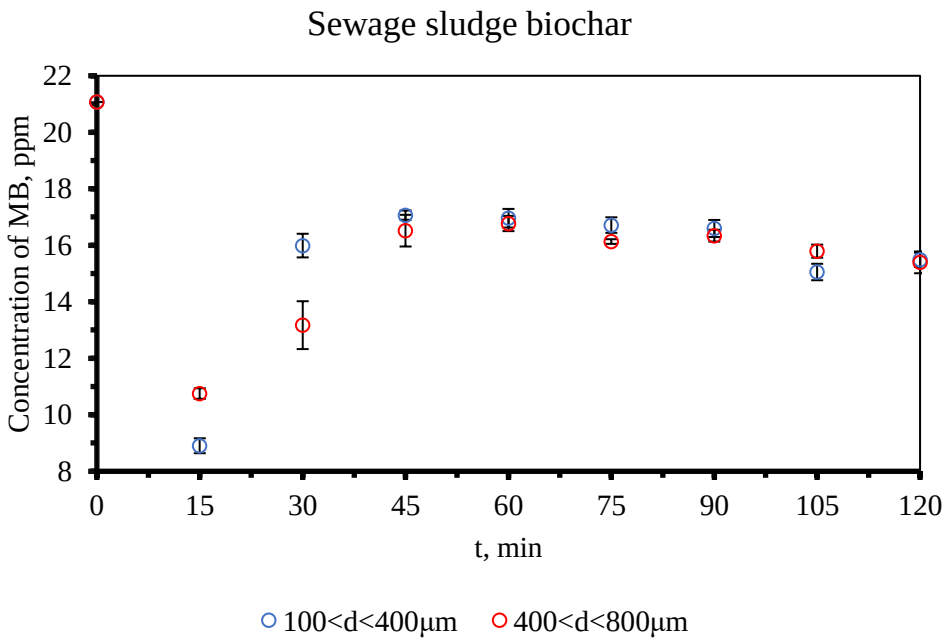

Figure 20. Methylene blue removal at 3 mg of the biochar and 15 mL MB solution.

Figure 21 showed the largest adsorption capacity of 0.058 at 15 min for 15 mL 20 ppm MB for 3 mg of sewage sludge biochar. After 15 min the adsorption capacity was decreased and the

total adsorption capacity was satisfying to a lower value than for 10 mg of sewage biochar of 25 mL 20 ppm MB solution.

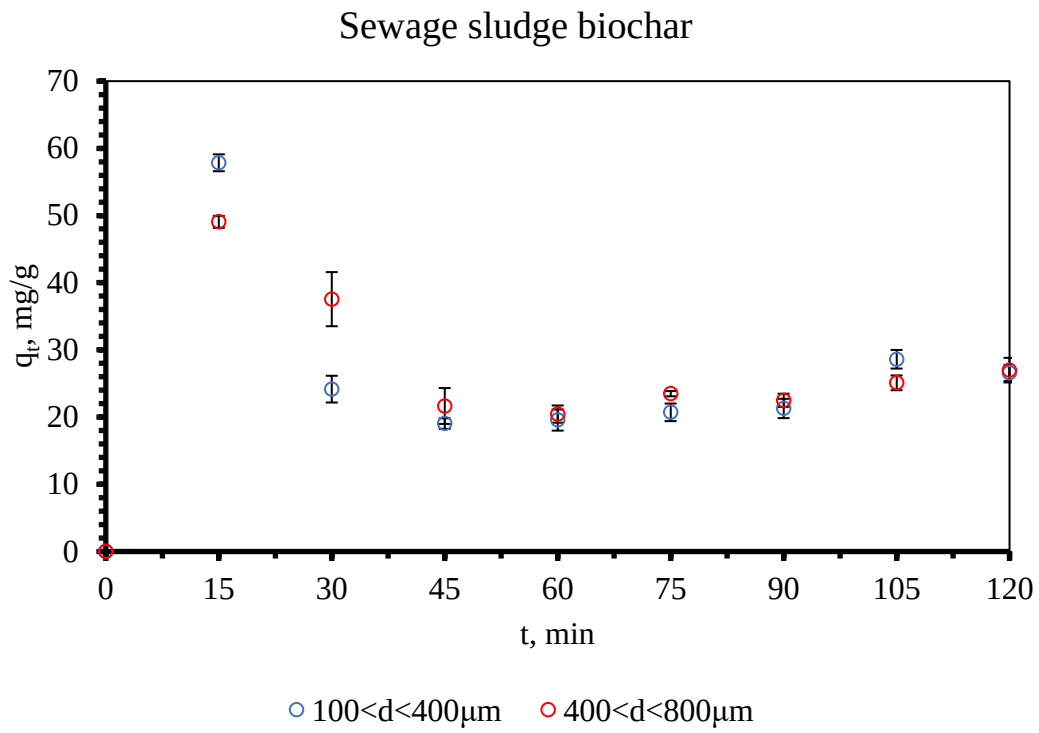

Figure 21. Adsorption capacity of sewage sludge biochar of 3 mg for 15 mL MB experiment.

Then it was estimated that a decrease in MB solution was not an effective way to control MB adsorption into sewage sludge biochar. Followed by increasing the weight load of sewage sludge biochar to 70 mg at 25 mL of 20 ppm MB solution. Observed results were demonstrated in Figures 22, 23, and 24.

MB adsorption at 70 mg of the sewage sludge biochar was reached before the adsorption efficiency of 34.4% at 60 min. At 15 min the adsorption efficiency was 25.6%. If compared with a 40 mg biochar weight load 70 mg had higher adsorption efficiency as 22.06% at 45 min was for 40 mg. In the case of 70 mg, at 45 min adsorption efficiency was 27.08% which was higher than the 40 mg adsorption test.

MB concentration reduction occurred in 15 minutes from 18.12 ppm to 13.48 ppm. The lowest concentration was 11.86 ppm at 60 min. Further occurred MB desorption to the inverse direction of the sorption experiment. Figure 24 showed the adsorption capacity of sewage sludge biochar which was 2.221 mg/g at 60 min for 70 mg of biochar which was lower than for 40 mg which was 2.596 mg/g. The increase in weight load was irreversible to the adsorption capacity of the sample.

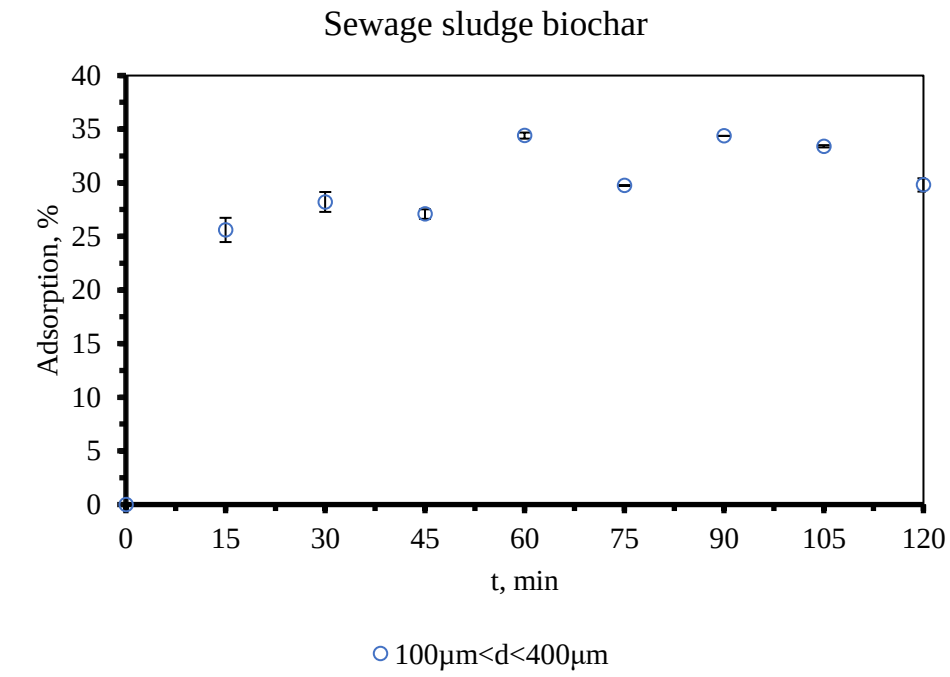

Figure 22. 70 mg weight load for 20 ppm MB removal and 25 mL of MB solution for 100 µm < d < 400 µm.

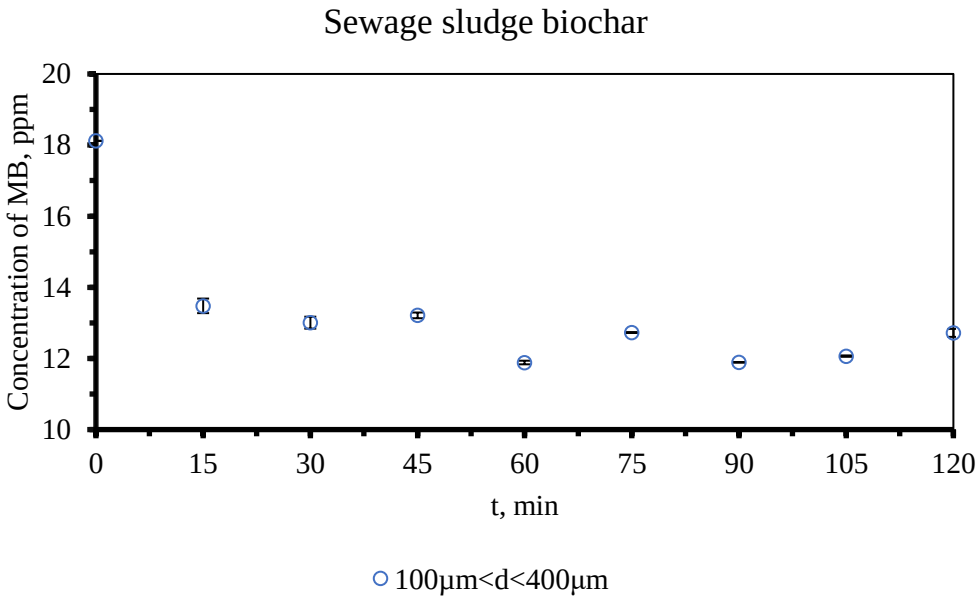

Figure 23. Methylene blue removal at 70 mg of the biochar.

Then for the check of adsorption way, it was completed a single test for an abbreviated time. The results were satisfied in Figures 25, 26, 27. The new sampling set showed that MB species were adsorbed immediately in 1min and then the limiting step was started.

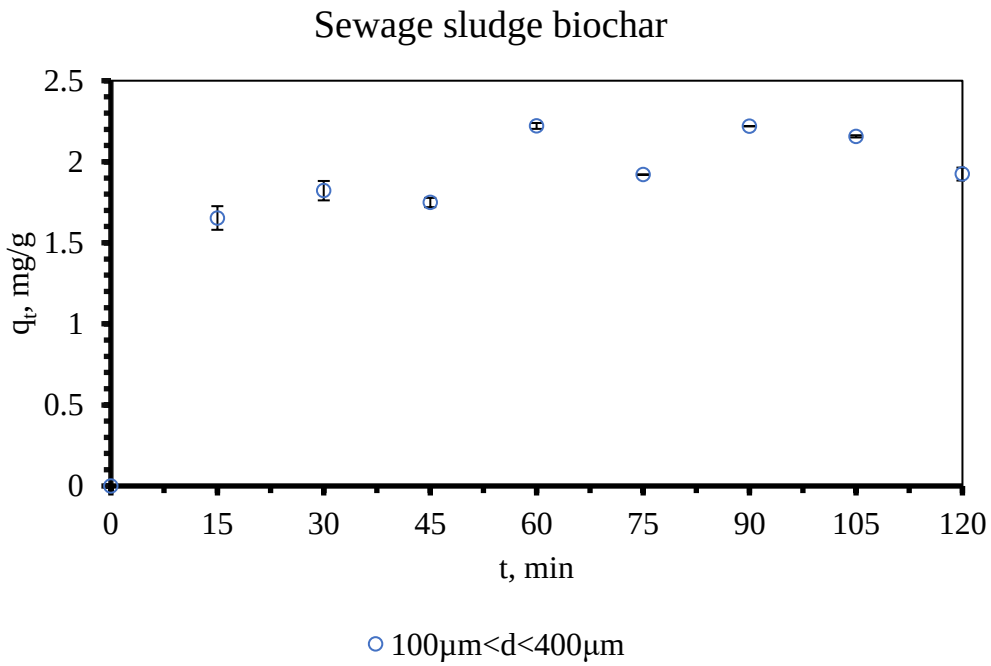

Figure 24. Adsorption capacity of sewage sludge biochar of 70 mg for 20 ppm MB experiment.

Figure 25 showed 16.08% adsorption efficiency in 1 minute and it reached 26.82% at 30min. The sampling times were satisfied at 0, 15, and 30 min and the behaviour was not changed. This test could describe the adsorption way of MB by sewage sludge biochar.

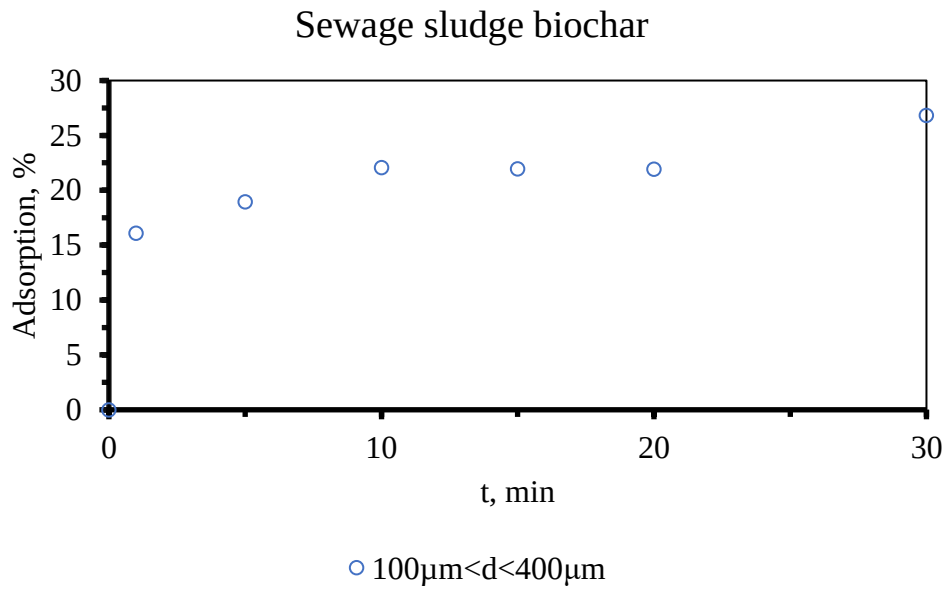

Figure 25. A single test of 70 mg biochar for 15 min efficiency check.

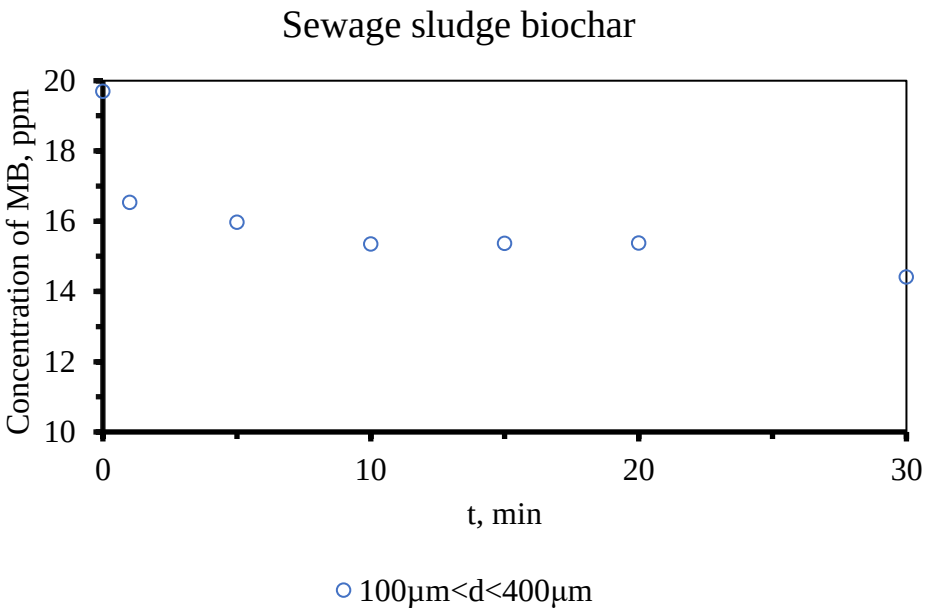

Figure 26. Methylene blue removal at 70 mg of the biochar by the single test with a new sampling set.

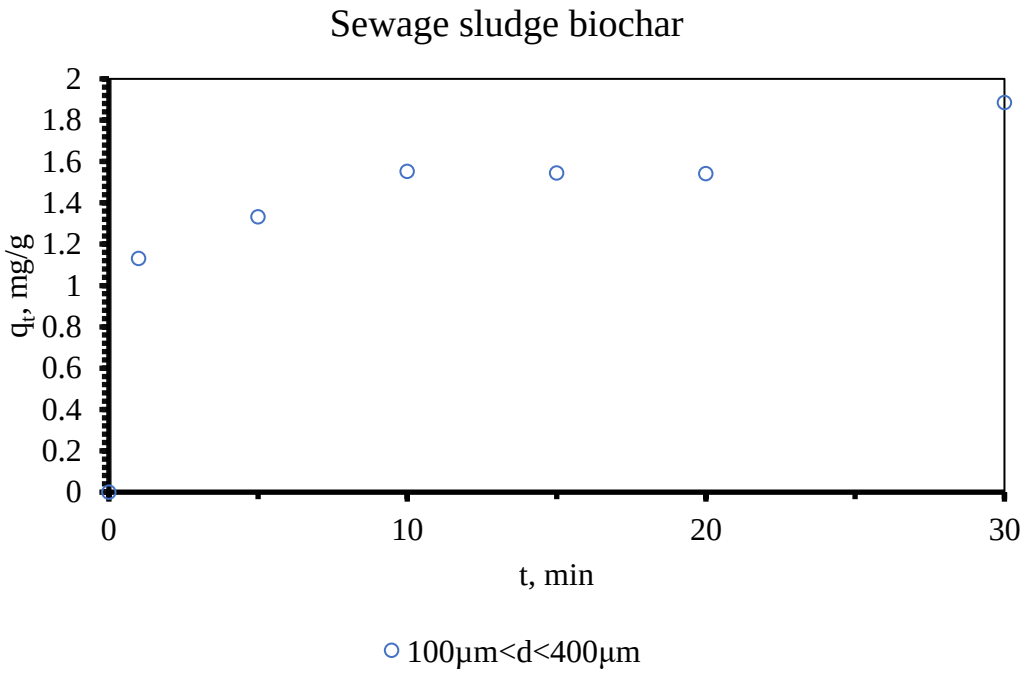

Figure 27. Adsorption capacity of 70 mg for a new sampling set.

The MB concentration reduction had the same behaviour as the double test for 2 hours. There were decreased to 16.53 ppm from 19.70 ppm in 1 min. Then at 30 min, it reached 14.42 ppm MB. The adsorption capacity of sewage sludge biochar was the same as in Figure 24 on the last sampling set. This single test was checked to evaluate the adsorption behaviour of MB by sewage sludge biochar.

With the new sampling set the adsorption experiment of double tests was conducted for 400 µm < d < 800 µm of sewage sludge biochar. The observed data was represented in Figures 28, 29, and 30.

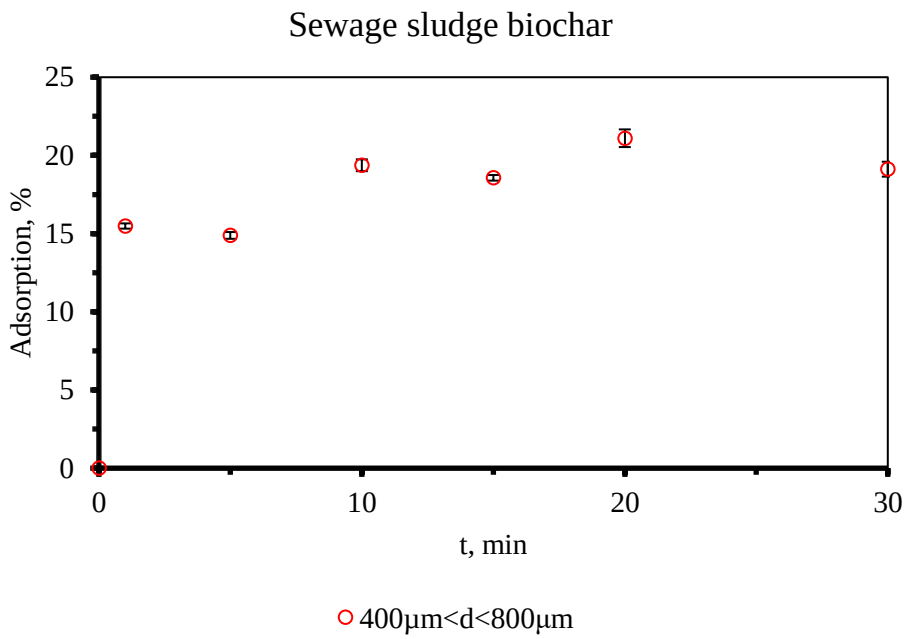

Figure 28. 70mg weight load for 20 ppm MB removal and 25 mL of MB solution for 400 µm < d < 800 µm.

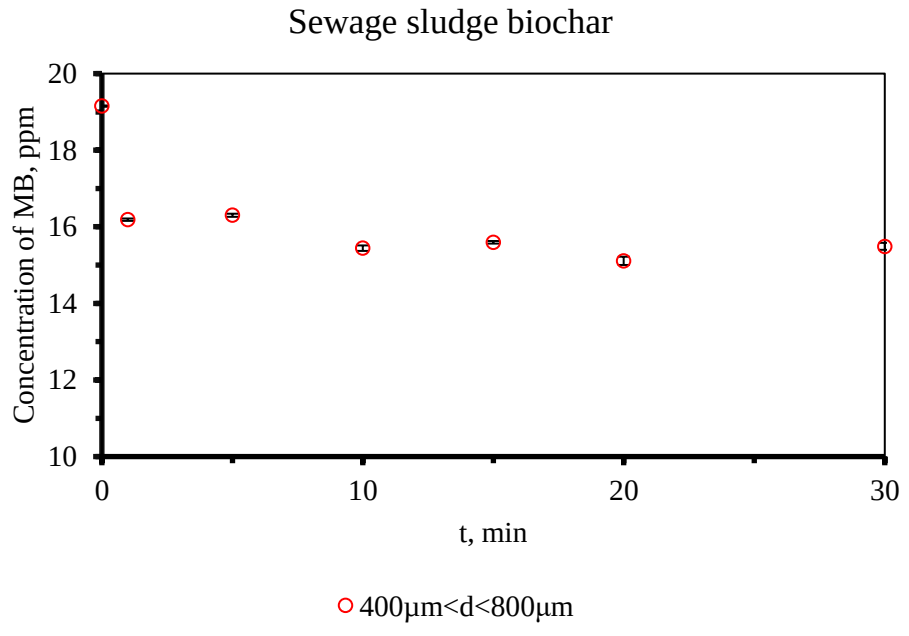

Figure 29. Methylene blue removal at 70 mg of the biochar.

The adsorption of MB with 70 mg of 400 µm < d < 800 µm size ranged sewage biochar was conducted only for 30 min satisfying the new sampling set. Figure 28 showed 15.48% adsorption efficiency in 1 min, and it reached 21.10% in 20 min. Comparatively to 100 µm < d < 400 µm it had a lower adsorption efficiency of the same weight load. 16.08% was satisfied for 1 min in the case of 100 µm < d < 400 µm, and 21.92% was at 20 min. The size effect on MB adsorption was also not so big for this weight load. Figure 29 showed the MB concentration reduction over time. And it reached 15.11 ppm at 20 min where the initial concentration was 19.15 ppm. Figure 30 an adsorption capacity of sewage sludge biochar of 400 µm < d < 800 µm particle size. The adsorption capacity in 1 min was 1.059 mg/g for 70 mg of 400 µm < d < 800 µm while for 100 µm < d < 400 µm was 1.131 mg/g for 70 mg. Comparatively 40 mg adsorption capacity was lower as it had about 2.092 mg/g for 15 min when 70 mg weight load showed 1.269 mg/g at 15 min.

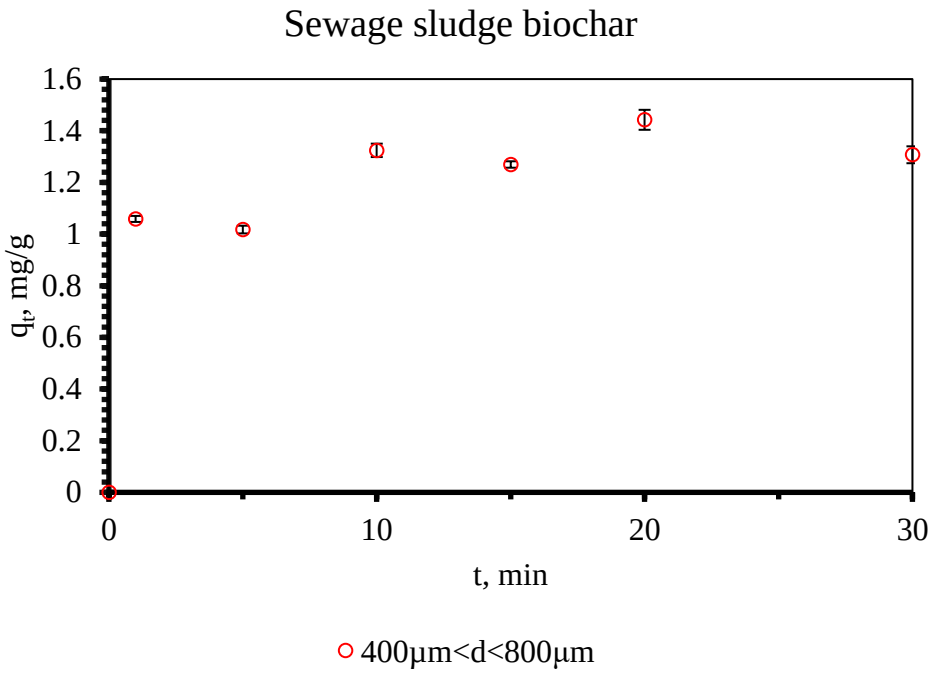

Figure 30. Adsorption capacity of 70 mg for 20 ppm MB solution.

The further weight load increase was applied to the new sampling set where 0, 1, 5, 10, 15, 20, and 30 minutes. Obtained and processed data were shown in Figures 31, 32, 33. In this data set were represented both particle size distributions of 100 µm < d < 400 µm and 400 µm < d < 800 µm ranges. Figure 31 showed the adsorption efficiency of 23.02% for 100 µm < d < 400 µm and 20.02% for 400 µm < d < 800 µm in 1 min. In the first sampling time, their differences were not big; however, in 30 min they had a larger difference. 100 µm < d < 400 µm showed 31.88% when 400 µm < d < 800 µm showed 25.70%.

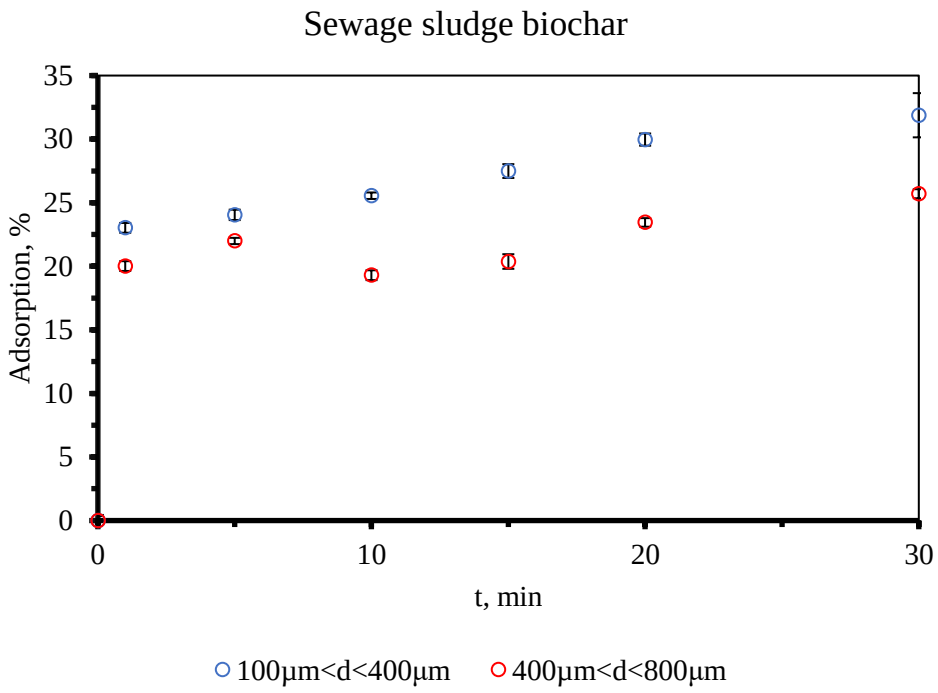

Figure 31. 100 mg weight load for 20 ppm MB removal.

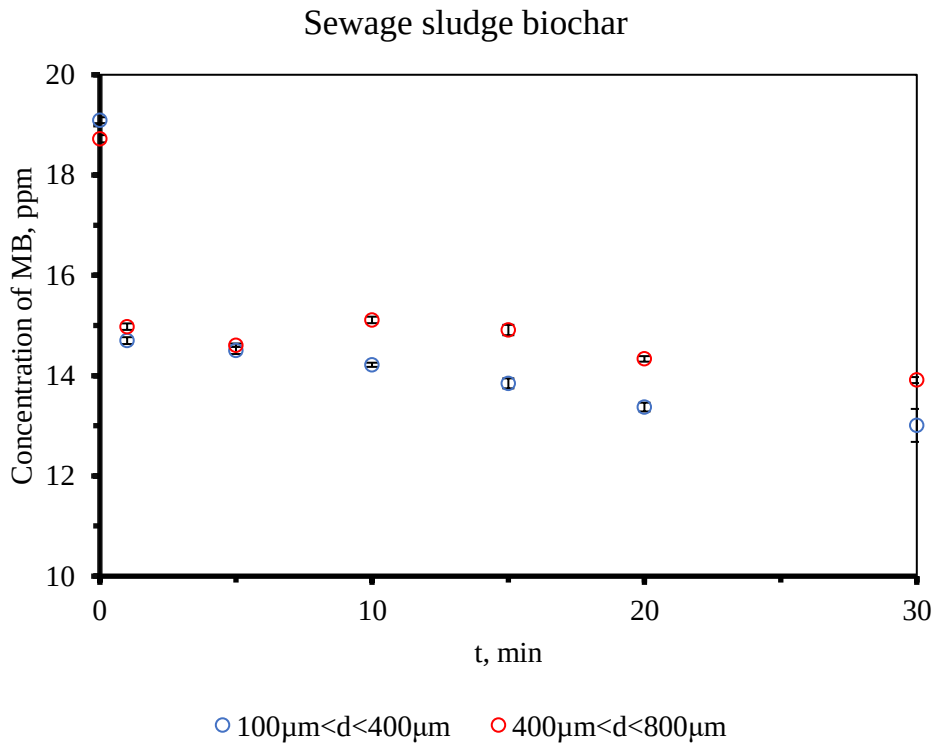

Figure 32. Methylene blue removal at 100 mg of the biochar.

Adsorption efficiency of sewage sludge biochars was increased comparatively to 70 mg weight load. 15.48% was for 400 µm < d < 800 µm in 1 min at 70 mg when 20.02% for 400 µm <

d < 800 µm at 100 mg. In the case of 100 µm < d < 400 µm was 16.08% at 70 mg and 23.02% at 100 mg in 1 min.

In Figure 32, MB concentration changed by spent time. In 1 min it was reduced to 14.70 ppm and in 30 min to 13 ppm for 100 µm < d < 400 µm. For another particle size distribution, MB reduction was 14.98 ppm in 1 min and 13.91 ppm in 30 min. The initial concentrations were 19.09 ppm and 18.72 ppm for 100 µm < d < 400 µm and 400 µm < d < 800 µm of sewage sludge biochar samples.

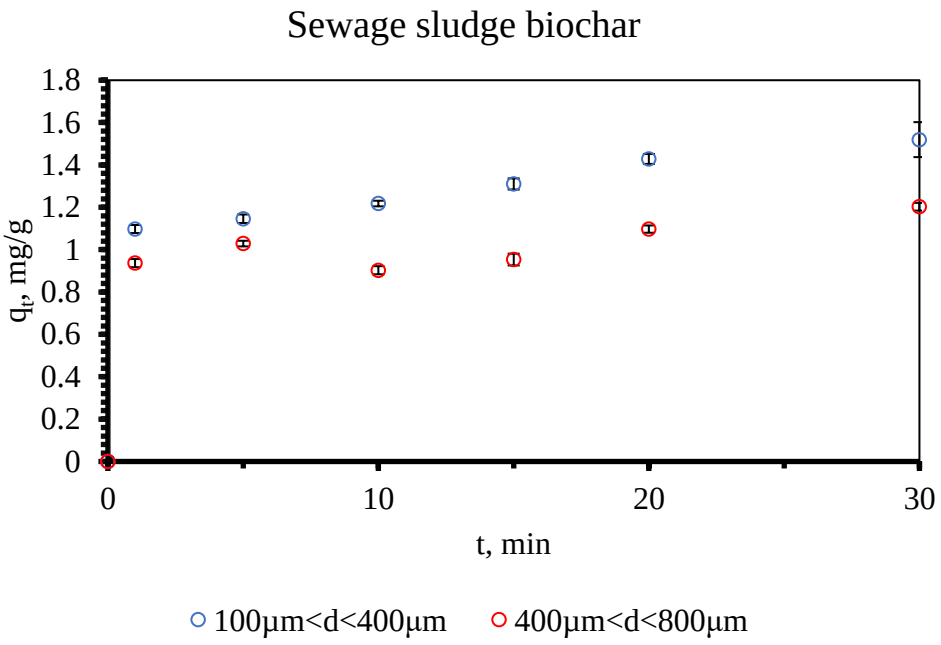

Figure 33. Adsorption capacity of 100 mg for 20 ppm MB experiment.

The adsorption capacity was low for 100 mg of sewage sludge biochar. In 1 min 1.097 mg/g was for 100 µm < d < 400 µm and 0.936 mg/g was for 400 µm < d < 800 µm. In 30 min it reached a slight increase to 1.520 mg/g for 100 µm < d < 400 µm and to 1.203 mg/g for 400 µm < d < 800 µm. Comparatively to 70 mg of sewage sludge biochar, the adsorption capacity was decreased slightly.

The sewage sludge biochar weight load was increased to 160 mg to evaluate the significant weight difference for 20 ppm MB adsorption experiments. The observed results were drawn from Figures 34, 35, and 36. In Figure 34, the adsorption efficiency change in 1 min as 400 µm < d < 800 µm was 23.76% when 100 µm < d < 400 µm was 17.62%. Before the weight load of 160 mg 100 µm < d < 400 µm always had a higher adsorption efficiency. However, after 1 min the adsorption behaviour of different particle sizes was followed regularly. At 30 min 23.23% was reached by 100 µm < d < 400 µm and 19.41% was for 400 µm < d < 800 µm. It was noticed that

the highest adsorption efficiency was achieved in 1 min, and it was decreased for 400 µm < d < 800 µm. The adsorption efficiency was higher than for 100 mg of sewage sludge biochar during MB removal. When 70 mg the adsorption efficiencies were 23.02% for 100 µm < d < 400 µm and 20.02% for 400 µm < d < 800 µm.

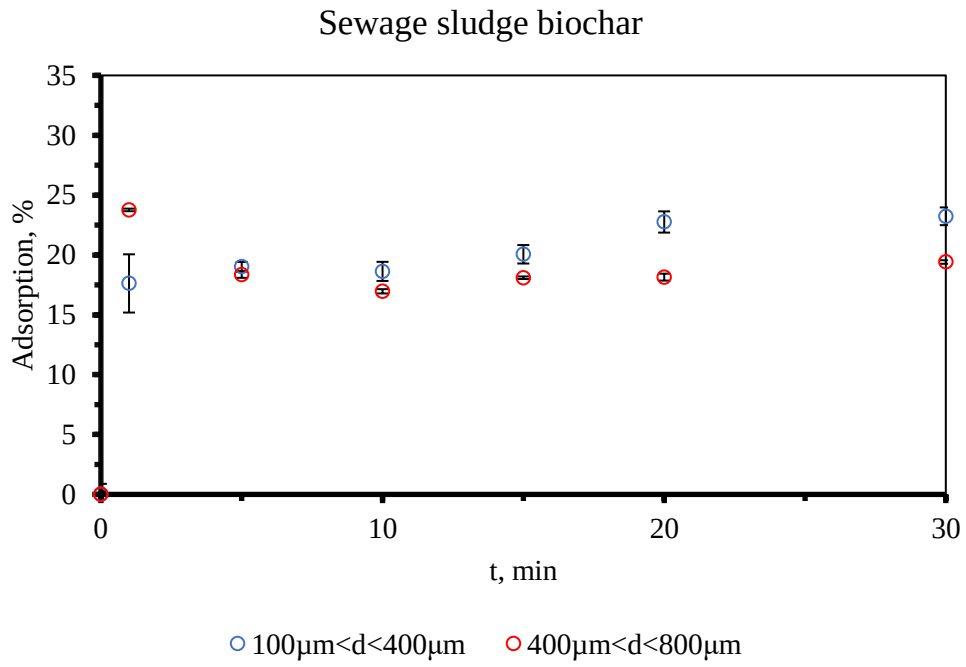

Figure 34. 160 mg weight load effect on the adsorption efficiency of MB.

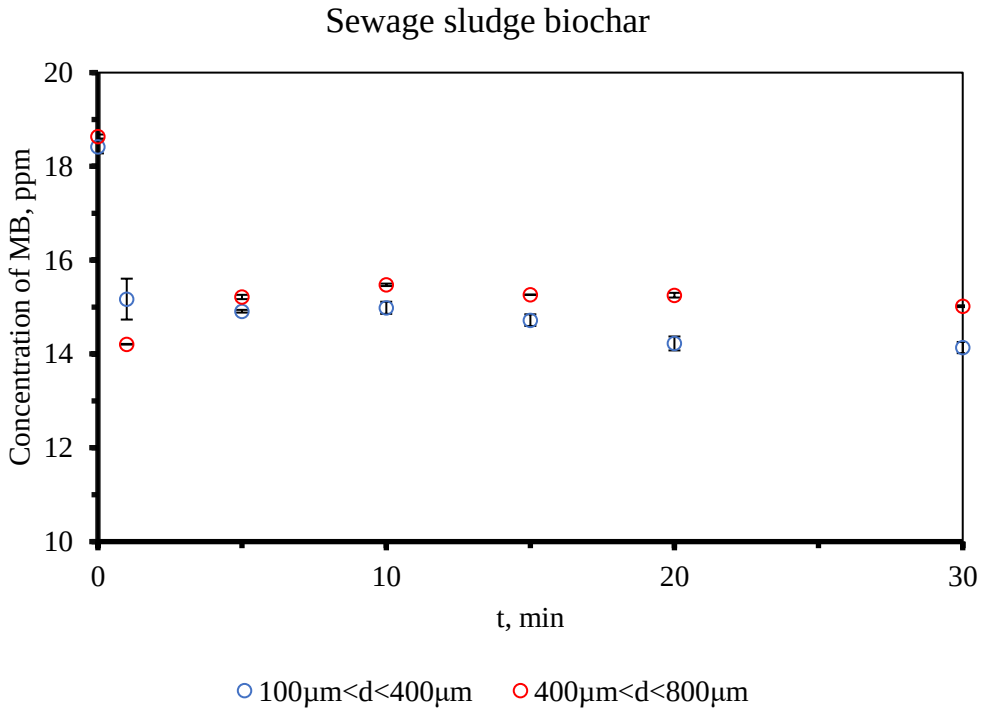

Figure 35. MB concentration changed by spending time at 160 mg weight load.

In Figure 35, MB concentration was reduced by spending time at 160 mg of sewage sludge biochar. As it was an irreversible graph for Figure 34 the changing tendency was clear. In 1 min it could be reduced to 14.21 ppm from 18.64 ppm for 400 µm < d < 800 µm sewage sludge biochar. For 100 µm < d < 400 µm was 15.17 ppm from 18.64 ppm of MB in 1 min.

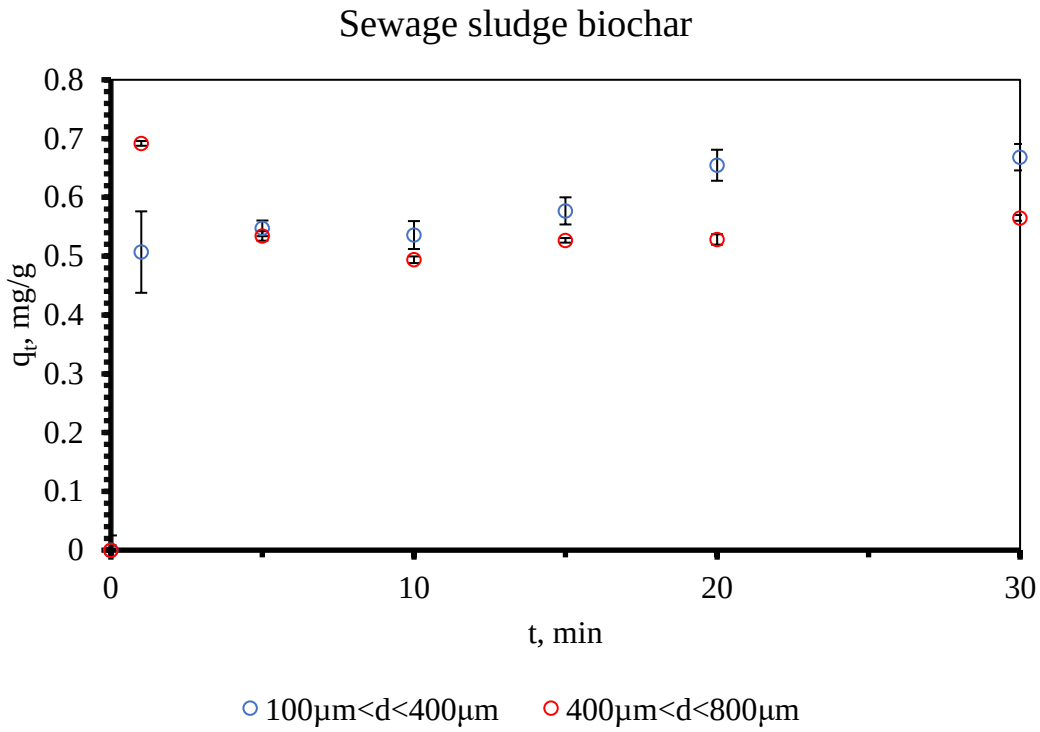

Figure 36. The adsorption capacity changed with time at 160 mg weight load of the biochar.

Figure 36 demonstrated the adsorption capacity of the sewage sludge biochar. It was lower for 160 mg compared to 100 mg. Further adsorption study was conducted for a 220 mg weight load of the sewage sludge biochar. The adsorption study results were given in Figures 37, 38, and 39.

The adsorption characteristics were different from previous graphs as in 30 min were not noticed desorption characteristics of MB. In 1 min adsorption efficiencies of both particle size biochars were similar. At 5 min the particle size effect was significantly changed. 100 µm < d < 400 µm had 21.35% and 400 µm < d < 800 µm had 15.66% in 5 min. In 30 minutes, the maximum adsorption efficiency was reached at 30.86% and 20.62%, respectively. The adsorption efficiency was higher for 220 mg than for 160 mg.

Figure 38 was given for MB removal of 220 mg of sewage sludge biochar. For 100 µm < d < 400 µm the final concentration at 30 min was 13 ppm whereas the initial concentration was 18.81 ppm. It was reduced to 14.60 ppm from 18.39 ppm in the application of 400 µm < d < 800

μm of sewage sludge biochar. The adsorption capacity graph was similarly interpreted to the adsorption efficiency. For 220 mg the adsorption capacity was decreased comparatively to 160 mg.

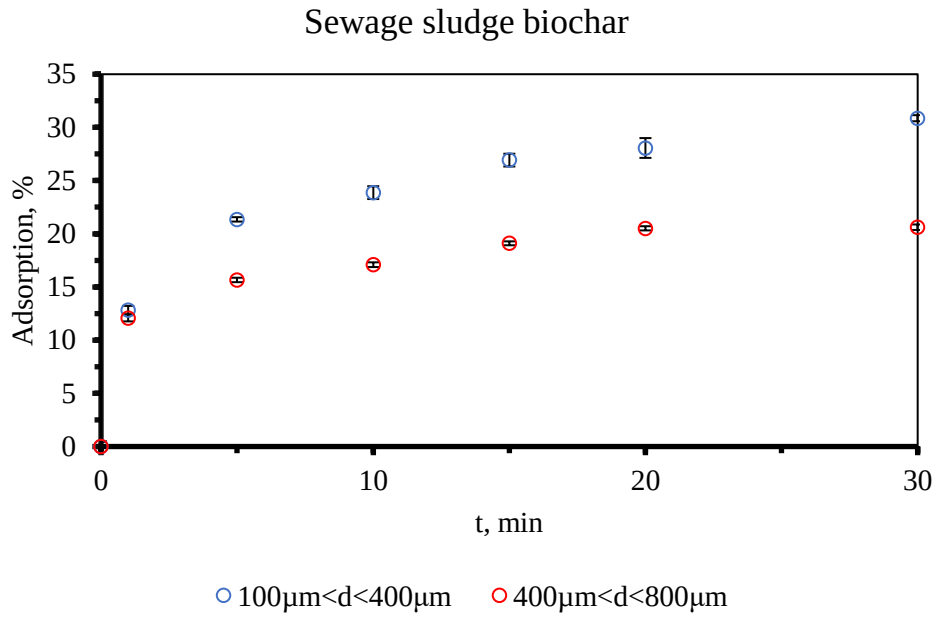

Figure 37. 220 mg weight load effect on the adsorption efficiency of MB.

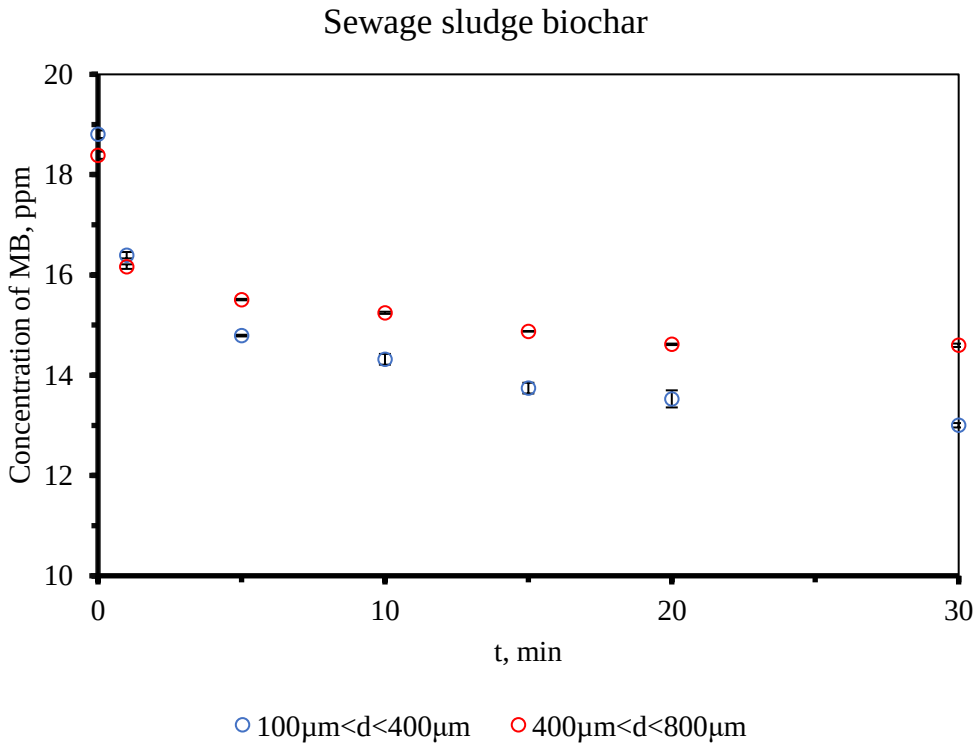

Figure 38. MB concentration changed by spending time at 220 mg weight load.

Figure 39 described that the adsorption capacity of the 100 µm < d < 400 µm sewage sludge biochar was higher than for 400 µm < d < 800 µm sewage sludge biochar. At 30 min was the highest adsorption capacity of 100 µm < d < 400 µm and it was 0.660 mg/g while 0.431 mg/g was for 400 µm < d < 800 µm. The capacity of adsorption was grown by spent time in the case of this weight load which was not noticed before.

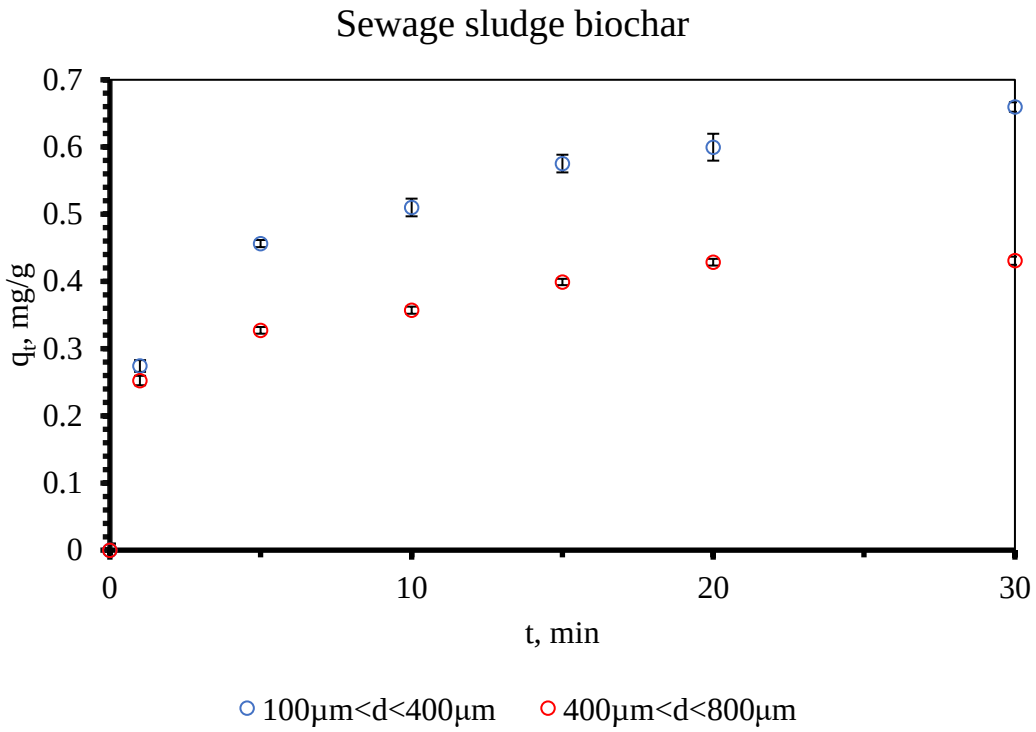

Figure 39. The adsorption capacity changed with time at 220 mg weight load of the biochar.

The sewage sludge biochar adsorption study was completed with the highest mass of 220 mg. Then it was turned to a straw flax biochar application for MB removal from an aquatic environment. Due to the limit of sample weight in this case were conducted three weight loads of the biochar. Weight loads were 100, 160, 220 mg of 100 µm < d < 400 µm, 400 µm < d < 800 µm. The other particle size distribution effects on the adsorption study were not considered as the sewage sludge biochar had only two size distributions. Followed that it was targeted to comparative analysis of both natures of biochar.

4.3.2 Methylene Blue removal by the adsorption of straw flax biochar

The straw flax biochar adsorption capacity and adsorption efficiency were studied by MB removal. The observed adsorption properties were represented in Figures 40, 41, and 42 for 100 mg in the short range for the check its removal way and were represented in Figures 43, 44, and 45 for 120 min with every 15 min sampling.

Figure 40 showed the adsorption efficiency tendency for the straw flax biochar of 100 mg for 20 ppm MB solution of 25 mL. On the graph was drawn that the active adsorption took place before 10 min and then it was started to limit the MB adsorption. The maximum adsorption efficiency was detected at 10 min for 100 µm < d < 400 µm which was 42.73%. In 1 min the adsorption efficiency for the same size distribution was 28.09%. At 30 minutes it was defined as 40.84% which meant the stable adsorption efficiency was reached 40%. In the case of 400 µm < d < 800 µm size range the adsorption efficiency was comparatively lower. In 1 minute, it reached 15.12% and the largest adsorption efficiency was detected at 20 minutes which was 25.22%.

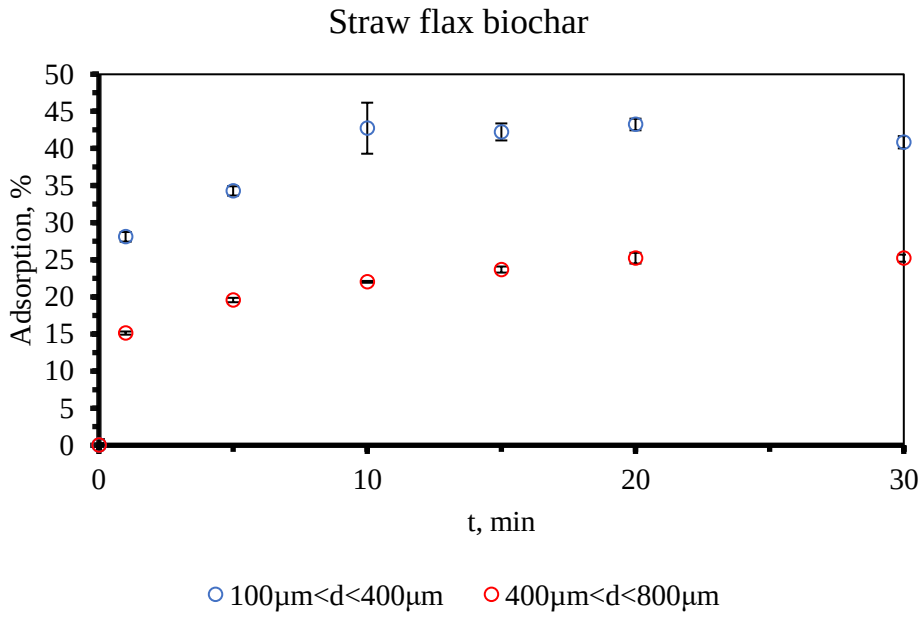

Figure 40. Adsorption efficiency of 100 mg of the straw flax biochar.

In Figure 41, the MB removal way for 100 mg of the straw flax biochar. Final concentrations at 30 min were 10.95 ppm and 14.50 ppm whereas initial concentrations were 18.51 ppm and 19.39 ppm, respectively. The adsorption was more effective with 100 µm < d < 400 µm than with 400 µm < d < 800 µm.

The sewage sludge biochar of 100 mg had an adsorption efficiency of 31.88% at 30 min while the straw flax biochar of 100 mg had an adsorption efficiency of 40.84% for 100 µm < d < 400 µm. There were noticed that the nature of the straw flax biochar was more advanced than the sewage sludge biochar for MB removal. It followed that the straw flax biochar had a higher adsorption capacity.

In Figure 42 the adsorption capacity of the straw flax biochar demonstrated that it had 1.974 mg/g at 10 min for 100 µm < d < 400 µm when it was 1.218 mg/g for 100 mg of the sewage sludge biochar of the same particle size range.

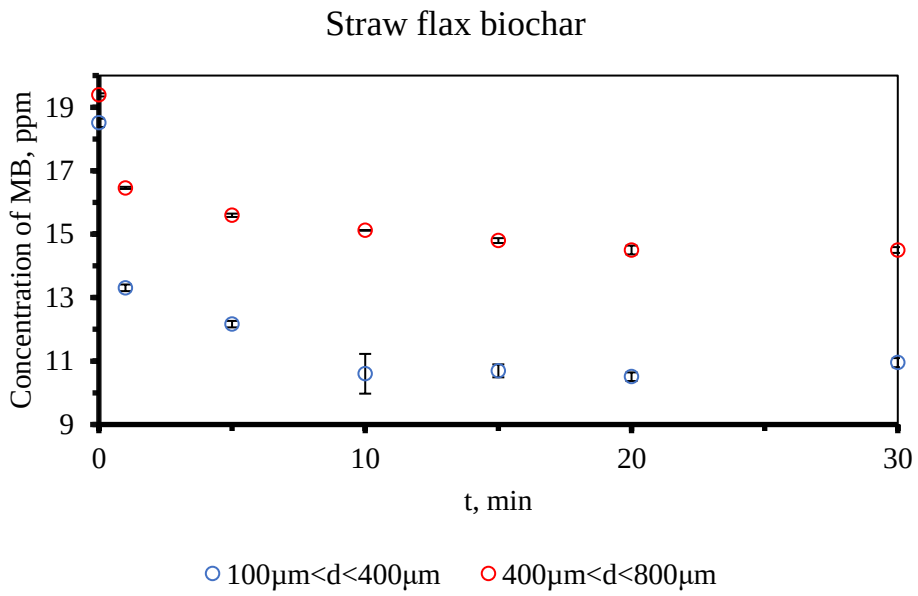

Figure 41. MB reduction by spending time for 100 mg of the straw flax biochar.

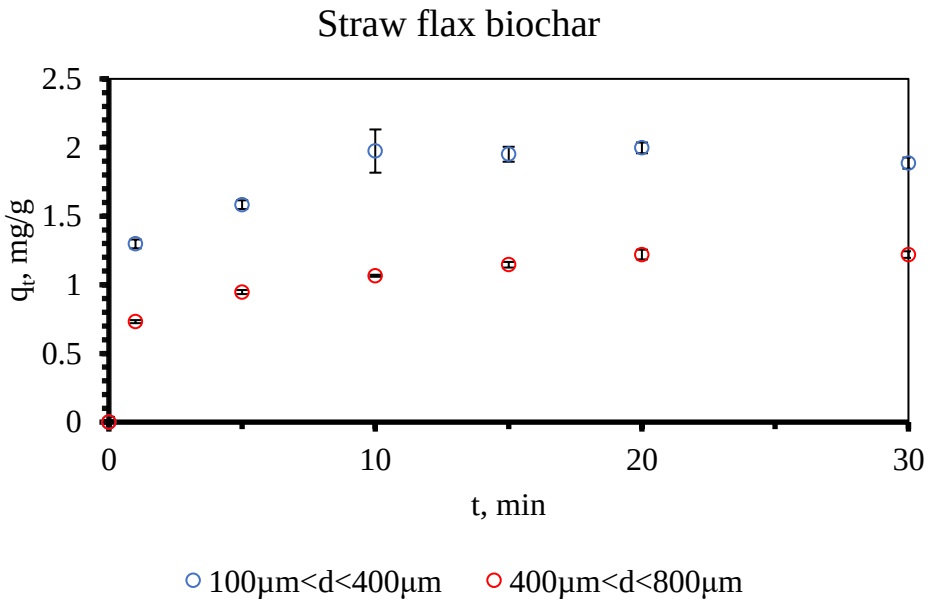

Figure 42. The adsorption capacity of 100 mg straw flax biochar for 20ppm MB removal.

The experiment's continuance for 2 hours was completed to be sure of the behaviour of the studying straw flax biochar adsorption properties and it was sampled every 15 min. It was described as possible to reach the adsorption efficiency to 51.16% in 2 hours for 100 µm < d < 400 µm straw flax biochar. In 2 hours, the adsorption efficiency of MB for 400 µm < d < 800 µm was achieved at 31.08%. In the 2 hours continuance of the experiment was noticed desorption of MB species was; however, due to the large amount of the straw flax biochar, it had small

desorption coeffects. The desorption coeffects were started at 30 min for 100 µm < d < 400 µm and at 45 min were started for 400 µm < d < 800 µm straw flax biochar. It meant that the increase in the weight load would stabilise the adsorption experiment for better MB removal.

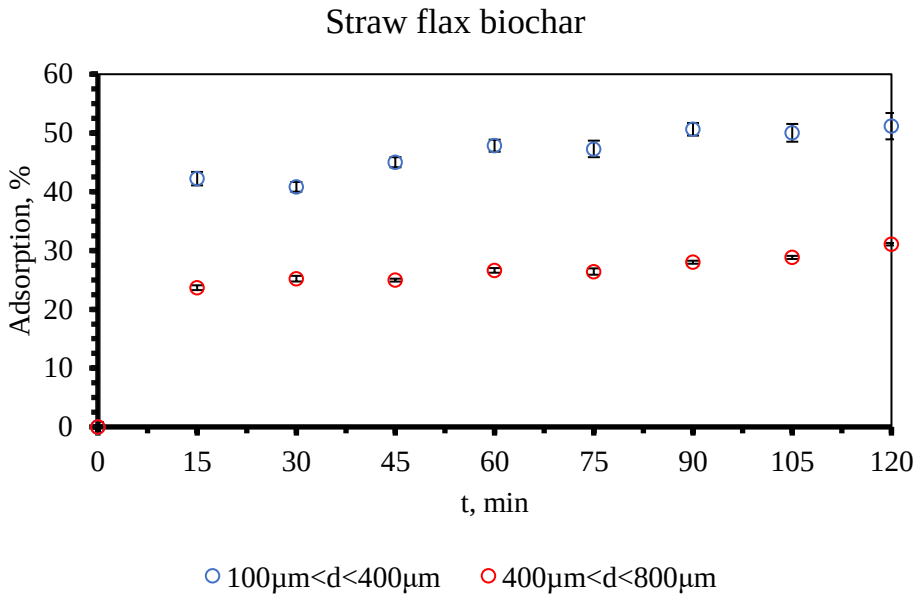

Figure 43. Adsorption efficiency of 100 mg of the straw flax biochar.

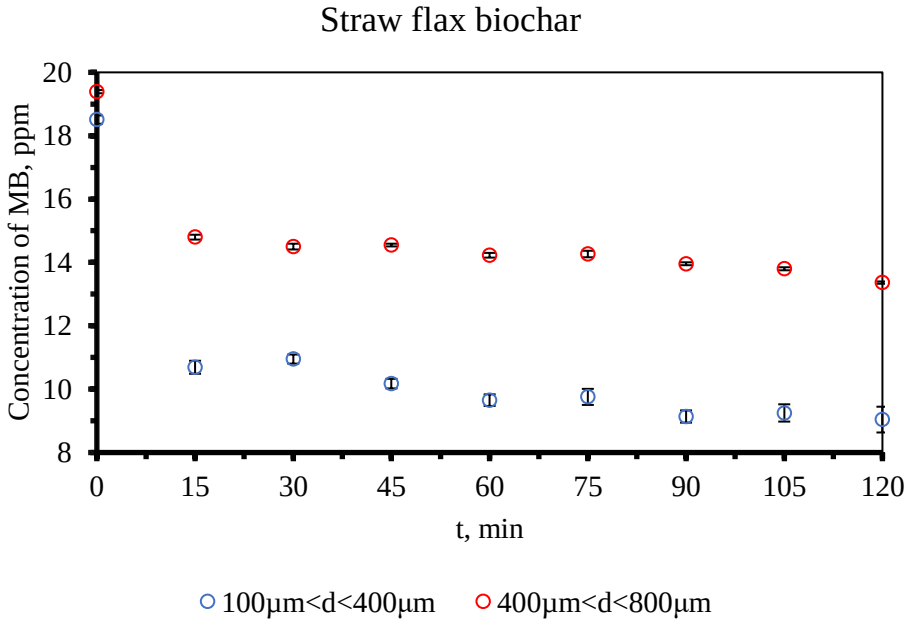

Figure 44. Adsorption efficiency of 100 mg of the straw flax biochar.

Figure 44 described the MB reduction by spent time. And final concentrations were 9.04 ppm and 13.36 ppm while the initial concentrations were 18.51 ppm and 19.39 ppm, respectively. The graph clearly described the limitation step of the adsorption experiment of MB removal.

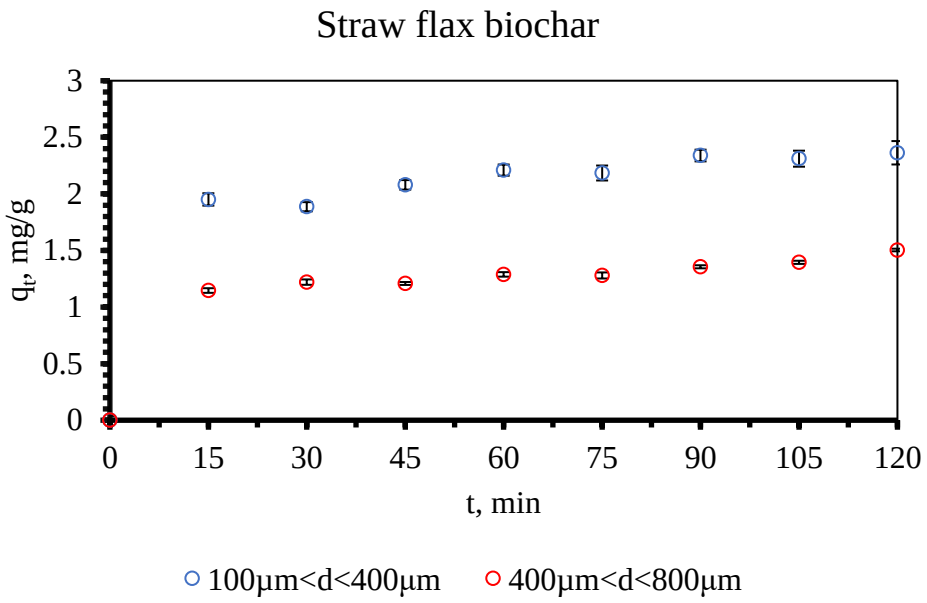

Figure 45. The adsorption capacity of 100 mg straw flax biochar for 20 ppm MB removal.

The adsorption capacity of straw flax biochar was higher than that of sewage sludge biochar. It was the graph for the approval of the adsorption efficiency and the tendency of the graph was similar. Then the weight load of the straw flax biochar was increased to 160 mg for 20 ppm MB adsorption experiments. The results were demonstrated in Figures 46, 47, and 48 for an abbreviated time and in Figures 49, 50, and 51 for the 2-hour continuance.

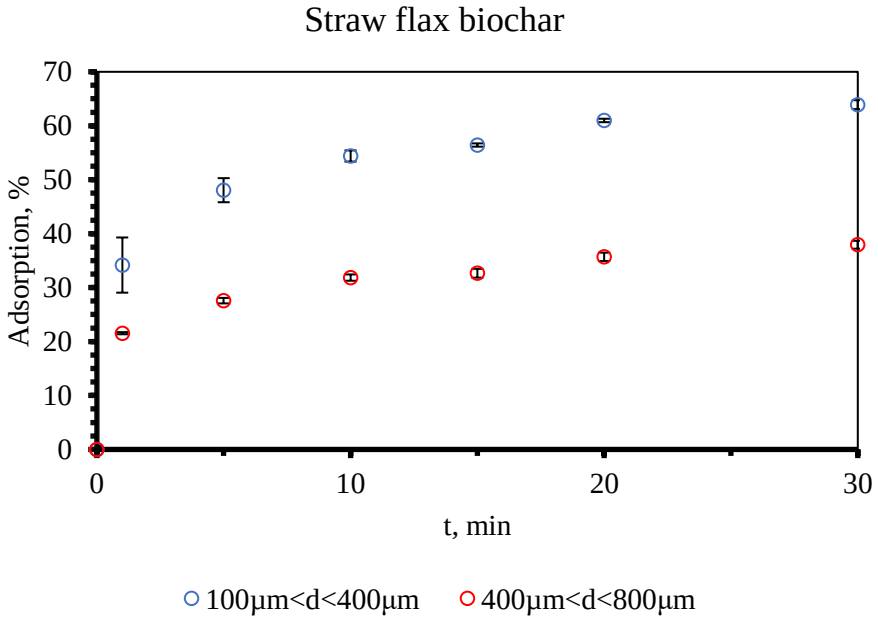

Figure 46. Adsorption efficiency of 160 mg of the straw flax biochar.

Figure 46, adsorption efficiencies of two different-sized straw flax biochar. In 30 min 100 µm < d < 400 µm achieved 63.92% and 400 µm < d < 800 µm achieved 37.94%. In 1 min 34.17% and 21.55%, respectively. The graph showed that in 30 minutes desorption coeffects were not noticed.

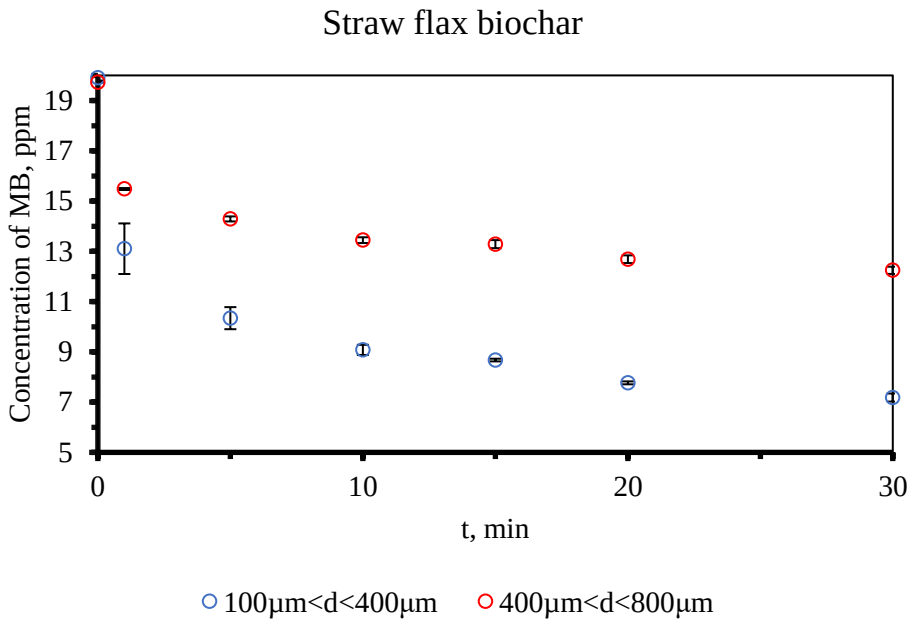

Figure 47. Adsorption efficiency of 160 mg of the straw flax biochar.

In Figure 47, the MB concentration reduction by time. In 30 min the MB concentration was decreased to 7.18 ppm from 19.91 ppm for 100 µm < d < 400 µm and was decreased to 12.25 ppm from 19.73 ppm for 400 µm < d < 800 µm. Comparatively to the sewage sludge biochar's 160 mg weight load experiment the straw flax biochar of 160 mg was advanced. 23.23% was adsorbed in 30 min by 100 µm < d < 400 µm of the sewage sludge biochar while 63.92% was adsorbed in the same period by 100 µm < d < 400 µm of the straw flax biochar 19.41% was adsorbed in 30 min by 400 µm < d < 800 µm of the sewage sludge biochar while 37.94% was adsorbed in the same period by 400 µm < d < 800 µm of the straw flax biochar.

The adsorption capacity of 160 mg straw flax biochar was 1.986 mg/g for 100 µm < d < 400 µm in 30 min. At the same time and with the same particle size distribution, the sewage sludge biochar had 0.668 mg/g of adsorption capacity. Comparatively, to 100 mg of the straw flax biochar, it was higher as 100 mg straw flax biochar's adsorption capacity was 1.886 mg/g when 160 mg was 1.986 mg/g for 100 µm < d < 400 µm of the straw flax biochar. The adsorption capacity of 400 µm < d < 800 µm for 160 mg was 1.168 mg/g in 30 min which meant that it had a lower adsorption capacity than 100 µm < d < 400 µm of the straw flax biochar. The adsorption capacity was increased by time and the difference between two particle sizes became significantly larger.

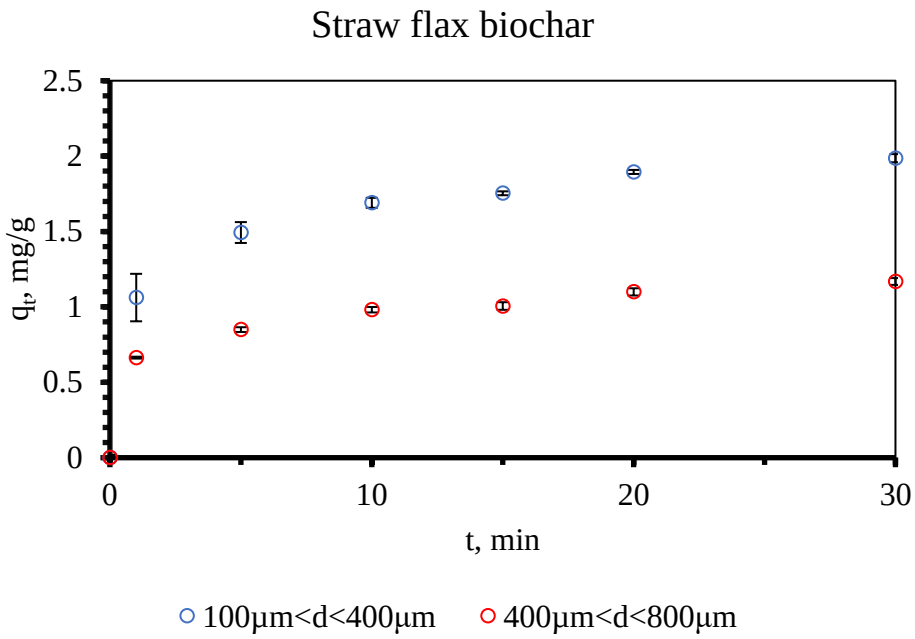

Figure 48. The adsorption capacity of 160 mg straw flax biochar for 20 ppm MB removal.

The continued further adsorption experiment for 2 hours was represented below, and it indicated that the limitation step without desorption coeffects occurred in this period. The adsorption efficiency difference became larger by spent time; however, in 2 hours 100 µm < d < 400 µm stopped to adsorb further the remaining MB which described the difference in adsorption efficiencies of two particle-sized biochar samples.

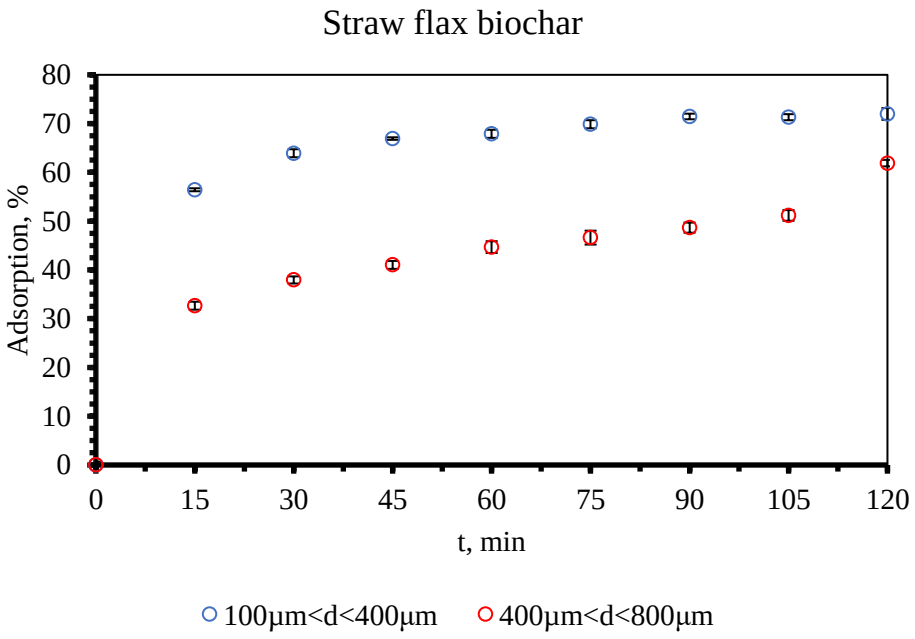

Figure 49. Adsorption efficiency of 160 mg of the straw flax biochar.

In 2 hours experiments the adsorption efficiency of 100 µm < d < 400µm was 71.97% which was achieved 71.46% in 90 min. The 400 µm < d < 800 µm straw flax biochar was achieved 61.89% in 120 min.

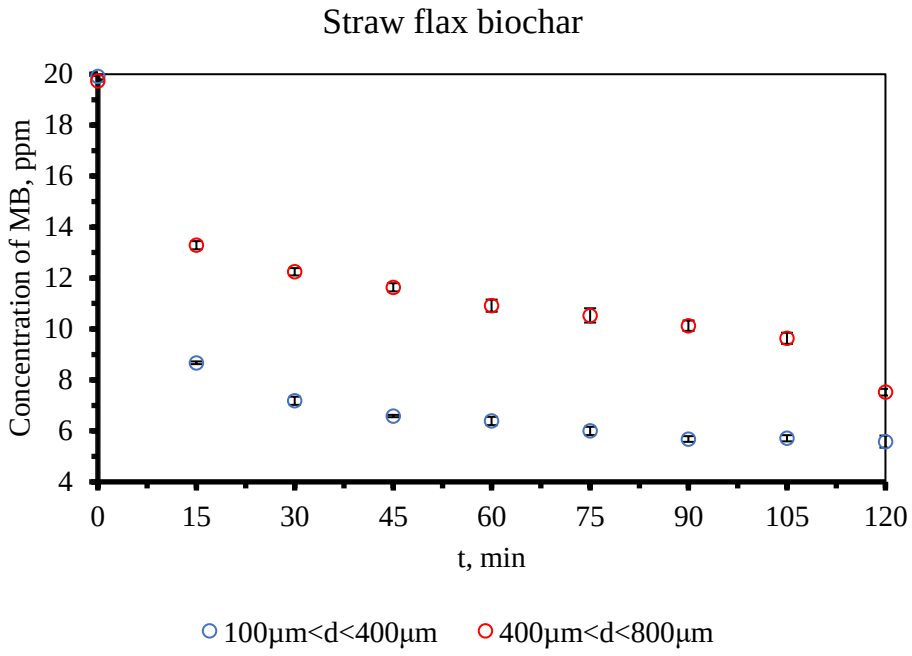

Figure 50. Adsorption efficiency of 160 mg of the straw flax biochar.

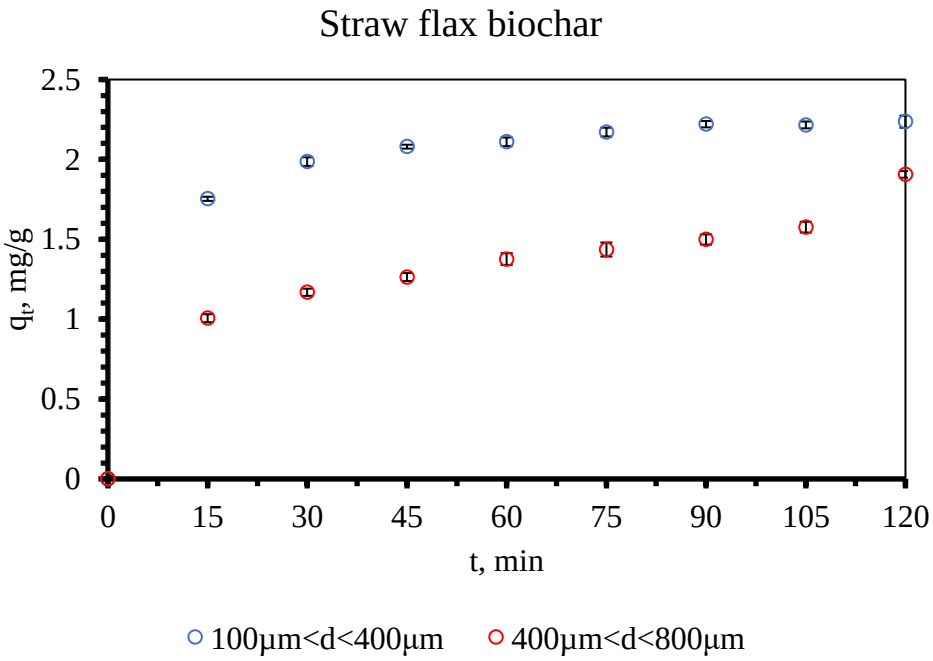

Figure 51. The adsorption capacity of 160 mg straw flax biochar for 20 ppm MB removal.

MB removal by the straw flax biochar of 160 mg was more effective than 100 mg of this biochar. Final concentrations were 5.58 ppm and 7.52 ppm at 30 min for 100 µm < d < 400 µm and 400 µm < d < 800 µm where were initial concentrations of 19.91 ppm and 19.73 ppm, respectively.

Adsorption capacities of straw flax biochar for 160 mg in 120 min were 2.236 mg/g for 100 µm < d < 400 µm and 1.906 mg/g for 400 µm < d < 800 µm. The adsorption capacity and the adsorption efficiency were described as the adsorption behaviour.

For the further adsorption check the weight load was increased to 220 mg. The satisfying results were drawn in Figures 52, 53, and 54 for abbreviated time and in Figures 55, 56, and 57 for the 2 hours continuance.

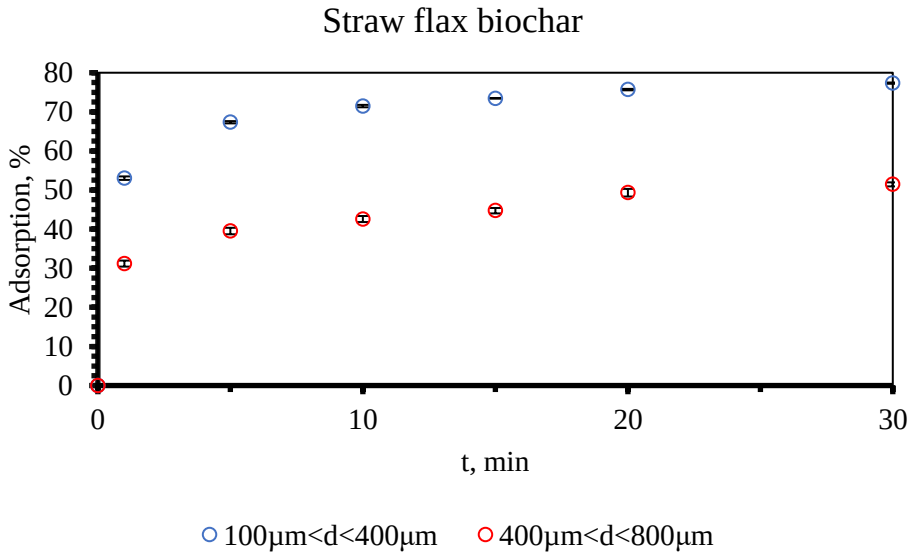

Figure 52. Adsorption efficiency of 220 mg of the straw flax biochar.

Figure 52 represented adsorption efficiencies of 100 µm < d < 400µm and 400 µm < d < 800 µm of the straw flax biochar during MB removal from the aquatic medium. The fast adsorption of MB species in 1 min were 53.03% for 100 µm < d < 400 µm and 31.19% for 400 µm < d < 800 µm. In 30 min 77.33% and 51.45%, respectively. In this period desorption coeffects were not detected which meant further adsorption of MB species. 220 mg of 100 µm < d < 400 µm straw flax biochar was more advanced than 160 mg 100 µm < d < 400 µm straw flax biochar as it reached 53.03% in 1 min when 160 mg had 34.17% in 1 min. In 30 minutes were 77.33% and 63.92%, respectively. Also, 220 mg of 100 µm < d < 400 µm straw flax biochar was more advanced than 220 mg of 100 µm < d < 400 µm sewage sludge biochar as in 1 min were 53.03% and 12.83%, respectively. In 30 minutes were 77.33% and 30.86%, respectively. The advanced adsorption efficiency of the straw flax biochar was studied further before 105 min.

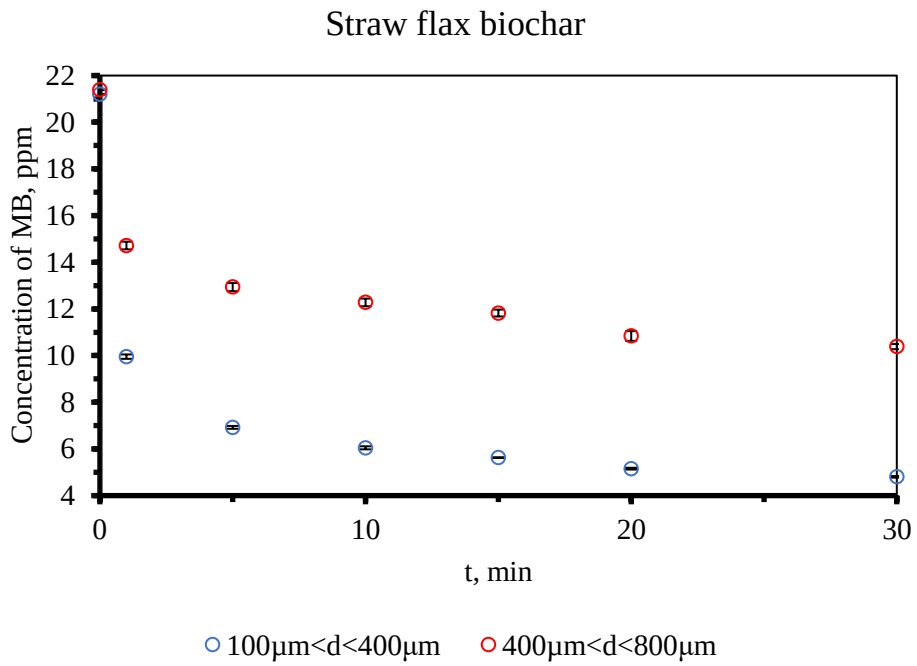

Figure 53. Adsorption efficiency of 220 mg of the straw flax biochar.

In Figure 53, MB concentration decreased with spent time through the application of the straw flax biochar. Initial concentrations for 100 µm < d < 400 µm and 400 µm < d < 800 µm were 21.20 ppm and 21.39 ppm, respectively. The final concentrations in 30 min were 4.8 ppm and 10.38 ppm, respectively.

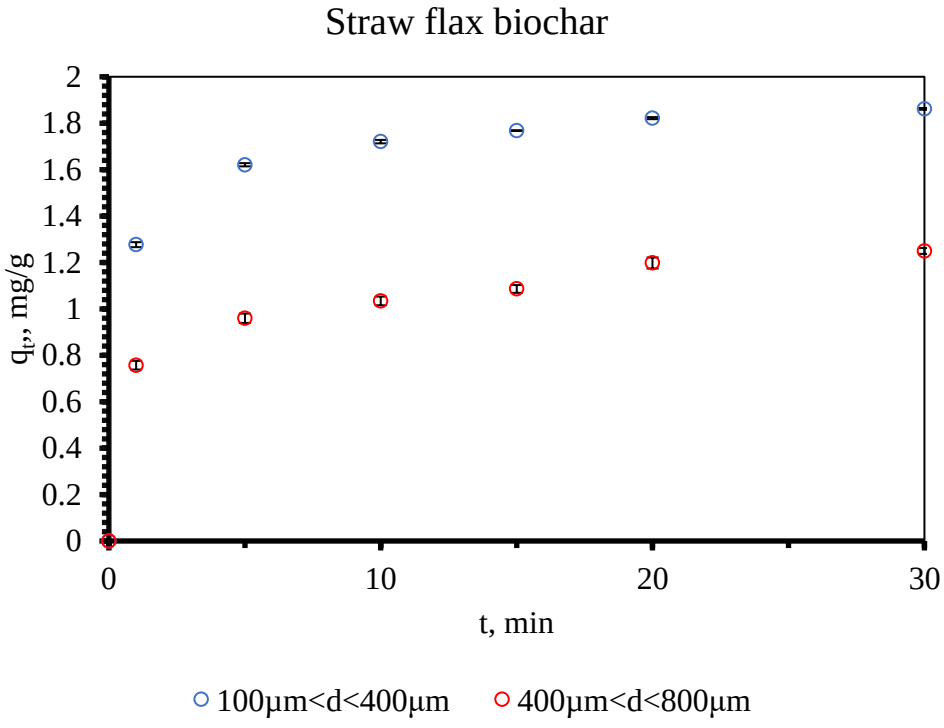

Figure 54. The adsorption capacity of 220 mg straw flax biochar for 20 ppm MB removal.

Figure 54 showed the adsorption capacities of the straw flax biochar samples of 100 µm < d < 400 µm and 400 µm < d < 800 µm sizes. Adsorption capacities at 30 min were 1.862 mg/g and 1.249 mg/g. Comparatively to 160 mg of the straw flax biochar's adsorption capacity of 100 µm < d < 400 µm size range 220 mg of the same size had a lower adsorption capacity as 160 mg had 1.986 mg/g; however, 400 µm < d < 800 µm straw flax biochar 220 mg had a higher adsorption capacity as 160 mg had 1.168 mg/g when 220 mg had 1.249 mg/g.

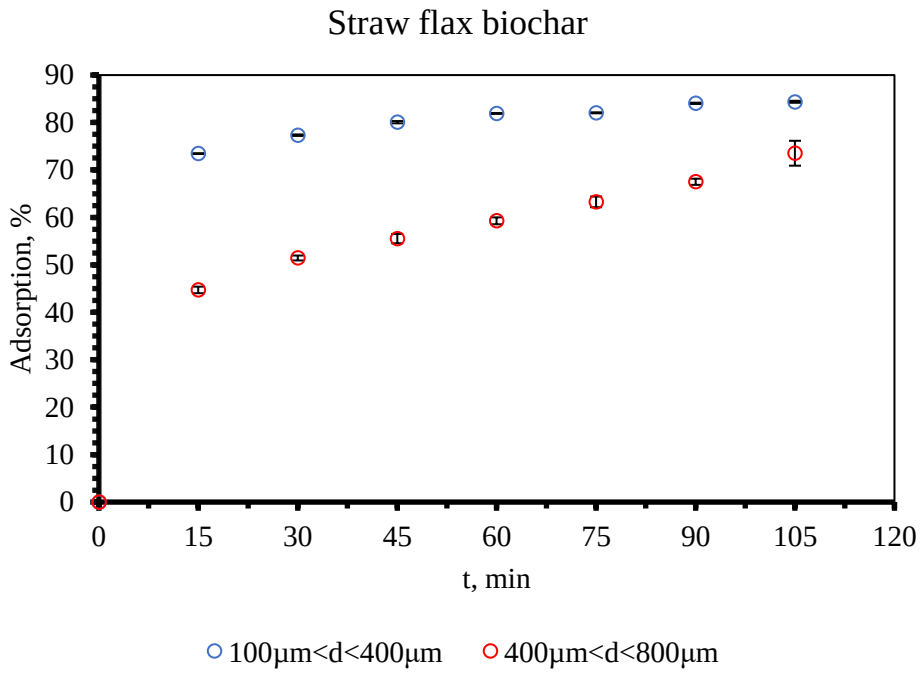

Figure 55. Adsorption efficiency of 220 mg of the straw flax biochar.

Figure 55 showed adsorption efficiencies of 100 µm < d < 400 µm and 400 µm < d < 800 µm of straw flax biochar during the continuance before 105 min. In 15 min adsorption efficiencies were 73.45% and 44.72%, respectively. In 105 min adsorption efficiencies were 84.37% and 73.52%, respectively. The adsorption efficiencies could be evaluated as a good adsorption property. From the graph was clear that after 90 min the limitation step occurred for 100 µm < d < 400 µm straw flax biochar. Comparatively 160 mg of straw flax biochar at 105 min 220 mg had a higher adsorption efficiency as 160 mg were 71.31% and 51.17% respectively to their size distribution.

Figure 56 described the MB removal way. Starting concentrations of 100 µm < d < 400 µm and 400 µm < d < 800 µm were 21.20 ppm and 21.39 ppm, respectively. In 105 min they became 3.31 ppm and 5.66 ppm, respectively. From the curve, they did not meet desorption coeffects during 105 min. In 15 minutes, they decreased to 5.63 ppm and 11.82 ppm, respectively.

In Figure 57 were manifested adsorption capacities of 100 µm < d < 400 µm and 400 µm < d < 800 µm for the straw flax biochar of 220 mg. In 105 min they achieved 2.031 mg/g and 1.786 mg/g, respectively. In 105 min 160 mg had 2.216 mg/g and 1.576 mg/g respectively, which meant 220 mg straw flax biochar was advanced.

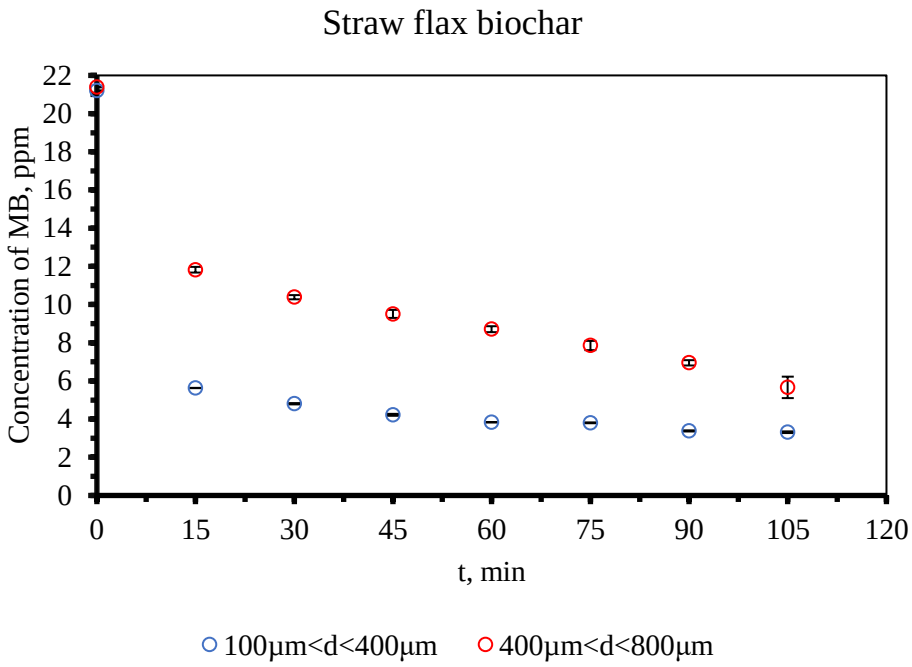

Figure 56. Adsorption efficiency of 220 mg of the straw flax biochar.

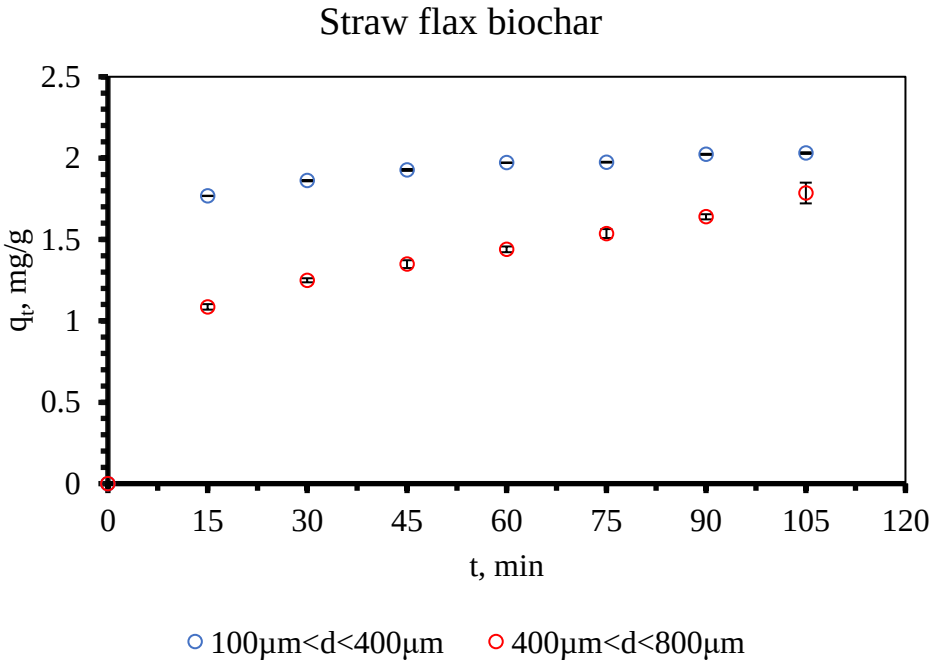

Figure 57. The adsorption capacity of 220 mg straw flax biochar for 20 ppm MB removal.

4.3.3 Total Methylene Blue removals comparison of two waste-derived biochars

The discussed data on MB adsorption experiments could be expressed in Table 9 for a concise data representation.

Table 9. Concise data representation of MB adsorption efficiencies for 20ppm MB.

#	The nature of the biochar	The particle size distribution	The weight load, mg	Adsorption time, min	Adsorption efficiency, %
1	2	3	4	5	6
1	The sewage sludge biochar	100 µm < d < 400 µm	10	120	15.07
2		400 µm < d < 800 µm		120	11.89
3		100 µm < d < 400 µm	40	120	21.09
4		400 µm < d < 800 µm		120	17.32
5		100 µm < d < 400 µm	70	30	26.82
6		400 µm < d < 800 µm		30	19.12
7		100 µm < d < 400 µm	100	30	31.88
8		400 µm < d < 800 µm		30	25.70
9		100 µm < d < 400 µm	160	30	23.23
10		400 µm < d < 800 µm		30	19.41
11		100 µm < d < 400 µm	220	30	30.86
12		400 µm < d < 800 µm		30	20.62
13	The straw flax biochar	100 µm < d < 400 µm	100	120	51.16
14		400 µm < d < 800 µm		120	31.08
15		100 µm < d < 400 µm	160	120	71.97
16		400 µm < d < 800 µm		120	61.89
17		100 µm < d < 400 µm	220	105	84.37
18		400 µm < d < 800 µm		105	73.52

Table 9 collected the final adsorption efficiencies of all experiments by spent time. It contained the nature of the biochar and its particle size distribution, and the weight load of adsorbents for data clarity.

From Table 9, it was noticed the advantage of the straw flax biochar comparatively to the sewage sludge biochar for the methylene blue removal experiments considering their nature and compositions. At the same time, there were shown the particle size effect on the adsorption behaviour was 100 µm < d < 400 µm more efficient for the methylene blue removal for both waste-derived biochars. The optimal weight load was 220 mg of the waste-derived biochar for 10 minutes of contact time for 20 ppm Methylene Blue solution.

Chapter 5. Conclusion

Methylene Blue adsorption from aquatic medium through the application of several hydrophobic natured biochar's was conducted and described. From Chapter 4 it might be concluded as follows:

1. FTIR analysis of both biochars approved the hydrophobic nature by the presence of functional groups: -CH=CH_2, -O-C=O. TGA analyses manifested that the best thermal tolerant sample was the straw flax biochar with PSD 400 μm < d < 800 μm, 72.40% of retained weight while the best thermal intolerance was demonstrated by the same sample with PSD 100 μm < d < 400 μm, 65.71% of retained weight at 800 ºC in the N_2 environment. SEM analysis results of the straw flax biochar with the magnification 5000 represented the microporous morphology comparatively to the sewage sludge biochar samples at the same magnification. XRD analysis observed data informed about the amorphous structural properties of biochar patterns as it did not show peaks for crystal lattices. The sewage sludge biochar with PSD 400 μm < d < 800 μm had several peaks which were not specific for crystal lattices.

2. PSD of two biochar samples separated samples for several size ranges. For straw flax biochar were separated for d < 100 μm – 2.483%, 100 μm < d < 400 μm – 27.605%, 400 μm < d < 800 μm – 50.135%, 800 μm < d < 1000 μm – 4.697%, 1000 μm < d – 15.08%. For sewage sludge biochar it was separated only for 100 μm < d < 400 μm – 39.816%, 400 μm < d < 800 μm – 60.184%.

3.1. The straw flax biochar was more advanced than the sewage sludge biochar for MB removal.

3.2. The PSD of 100 μm < d < 400 μm was more effective than 400 μm < d < 800 μm.

3.3. The observed maximum adsorption efficiency was 53.03% in 1 min.

3.4. The observed maximum adsorption efficiency was 84.37% in 105 min.

3.5. The considered maximum weight load was 220 mg for 20 ppm MB solution.

Advantages of this study. The application of the waste material of the pyrolysis. The available and cheap adsorbent for the water treatment directions. The fast adsorption of pollutants in 10 min.

Limitations of the biochar applications. The weight load of adsorbent in the solution. The PSD effect on the adsorption efficiency.

Future perspectives of this study are in the application of those biochar materials for the removal of other organic pollutants from contaminated water. The main significance is that the second life of waste materials for water treatment as an adsorbent satisfying the circular economy.

References

Abdelfatah, A. M., Fawzy, M., Eltaweil, A. S., El-Khouly, M. E. (2021). Green Synthesis of Nano-Zero-Valent Iron Using Ricinus Communis Seeds Extract: Characterisation and Application in the Treatment of Methylene Blue-Polluted Water. *ACS Omega, 6, 25397-25411*. doi: 10.1021/acsomega.1c03355

Bibi, S., Ullah, R., Burni, T., Ullah, Z., Kazi, M. (2023). Impact of Resorcinol and Biochar Application on the Growth Attributes, Metabolite Contents, and Antioxidant Systems of Tomato (*Lycopersicon esculentum Mill.*). *ACS Omega*, 8, 45750-45762. doi: 10.1021/acsomega.3c06233

Buss, W., Bogush, A., Ignatyev, K., Masek, O. (2020). Unlocking the Fertilizer Potential of Waste-Derived Biochar. *ACS Sustainable Chem. Eng.*, 8, 12295-12303. doi: 10.1021/acssuschemeng.0c04336

Chakraborty, A., Adhikary, S., Bhattacharya, S., Dutta, S., Chatterjee, S., Banerjee, D., Ganguly, A., Rajak, P. (2023). Pharmaceuticals and Personal Care Products as Emerging Environmental Contaminants: Prevalence, Toxicity, and Remedial Approaches. *ACS Chemical Health & Safety*, 30 (6), 362-388. doi: 10.1021/acs.chas.3c00071

Chou, K., McCaffrey, Z., Klamczynski, A. P., Torres, L. F., Compton, D. L., Glenn, G., Hart-Cooper, W. M. (2024). Biodegradation Rates of Ferulic Acid Derivatives and Traditional Sunscreen Actives in Marine, Bay, and Freshwater Environments. *ACS Sustainable Chem. Eng.*, 12 (10), 3899-3908. doi: 10.1021/acssuschemeng.3c05002

Crystal Impact. (2023, November). Match! Phase analysis using powder diffraction. Retrieved from https://www.crystalimpact.com/match/

Doble, J., Wilson, G., Wainman, J. W. (2023). Kinetic and Thermodynamic Analysis of the Adsorption of Methylene Blue onto Biochar. *J. Chem. Educ.*, 100, 4040-4046. doi: 10.1021/acs.jchemed.3c00518

Gai, S., Zhang, J., Fan, R., Xing, K., Chen, W., Zhu, K., Zheng, X., Wang, P., Fang, X., Yang, Y. (2020). Highly Stable Zinc-Based Metal-Organic Frameworks and Corresponding Flexible Composites for Removal and Detection of Antibiotics in Water. *ACS Applied Materials & Interfaces*, 12 (7), 8650-8662. doi: 10.1021/acsami.9b19583

Igalavithana, A. D., You, S., Zhang, L., Shang, J., Lehmann, J., Wang, X., Zhu, Y.-G., Tsang, D. C. W., Park, Y.-K., Hou, D., Ok, Y. S. (2022). Progress Barriers, and Prospects for Achieving a "Hydrogen Society" and Opportunities for Biochar Technology. *ACS EST Engg.*, 2, 1987-2001. doi: 10.1021/acsestengg.1c00510

Jiang, S.-F., Sheng, G.-P., Jiang, H. (2019). Advanced in the Characterization Methods of Biomass Pyrolysis Products. *ACS Sustainable Chem. Eng.*, 7, 12639-12655. doi: 10.1021/acssuschemeng.9b00868

Joshi, M., Bhatt, D., Srivastava, A. (2023). Enhanced Adsorption Efficiency through Biochar Modification: A Comprehensive Review. *Industrial & Engineering Chemistry Research*, 62 (35), 13748-13761. doi: 10.1021/acs.iecr.3c02368

Lauro, F. D., Balsamo, M., Solimene, R., Alfieri, M. L., Manini, P., Migliaccio, R., Salatino, P., Montagnaro, F. (2024). Characterisation of Biocrude Produced by Hydrothermal Liquefaction of Municipal Sewage Sludge in a 500 mL Batch Reactor. *Industrial & Engineering Chemistry Research*, 63, 955-967. doi: 10.1021/acs.iecr.3c03058

Lopez, J. E., Builes, S., Saldago, M. A. H., Tarelho, L. A. C., Arroyave, C, Aristizabal, A., Chavez, E. (2020). Adsorption of Cadmium Using Biochars Produced from Agro-Residues. *J. Phys. Chem. C.*, 124, 14592-14602. doi: 10.1021/acs.jpcc.0c02216

Luyen, N. T., Nguyen, K. V., Dang, N. V., Huy, T. Q., Linh, P. H., Trung, N. T., Nguyen, V.-T., Thanh, D. V. (2023). Facile One-Step Pyrolysis of ZnO/Biochar Nanocomposite for Highly Efficient Removal of Methylene Blue Dye from Aqueous Solution. *ACS Omega*, 8, 26816-26827. doi: 10.1021/ acsomega.3c01232

Mochizuki, Y., Bud, J., Liu, J., Tsubouchi, N. (2020). Production of Silicone Tetrachloride from Rice Husk by Chlorination and Performance of Mercury Adsorption from Aqueous Solution of the Chlorinated Residue. *ACS Omega*, 5, 29110-29120. doi: 10.1021/acsomega.0c03789

Mukhambet, Y., Shah, D., Tatkeyeva, G., Sarbassov, Y. (2022). Slow pyrolysis of flax straw biomass produced in Kazakhstan: Characterisation of enhanced tar and high-quality biochar. *Fuel*, 324, 124676. doi: 10.1016/j.fuel.2022.124676

Navarathna, C. M., Dewage, N. B., Keeton, C., Pennisson, J., Henderson, R., Lashley, B., Zhang, X., Hassan, E. B., Perez, F., Mohan, D., Pittman, C. U., Mlsna, T., Mlsna, J. (2020). Biochar Adsorbent with Enhanced Hydrophobicity for Oil Spill Removal. *ACS Appl. Mater. Interfaces*, 12, 9248-9260. doi: 10.1021/acsami.9b20924

Osman, A. I., Young, T. J., Farrell, C., Harrison, J., Al-Muhtaseb, A. H., Rooney, D. W. (2020). Physicochemical Characterisation and Kinetic Modeling Concerning Combustion of Waste Berry Pomace. *ACS Sustainable Chem. Eng.*, 8 (47), 17573-17586. doi: 10.1021/acssuschemeng.0c07390

Radboud University Nijmegen (2023, November). Information on the FESEM (Field-emission Scanning Electron Microscope). Retrieved from https://www.vcbio.science.ru.nl/public/pdf/fesem_info_eng.pdf

Shi, C., Wang, T., Roy, S., Chopra, S. S., Chen, G., Shang, J., Tian, J., Ok, Y. S. (2023). From Waste to Resource: Surface-Engineered Spent Coffee Grounds as a Sustainable Adsorbent for Oil-Water Separation. ACS EST Engg., 3, 1297-1307. doi: 10.1021/acsestengg.3c00096

Song, G., Zhao, L., Zhao, H., Xiao, J., Wang, H., Guo, S. (2020). Design and Assessment of a Novel Cogeneration Process of Synthetic Natural Gas and Char via Biomass Pyrolysis – Coupled Hydrothermal Gasification. *Ind. Eng. Chem. Res.*, 59, 22205-22214. doi: 10.1021/acs.iecr.0c04504

Tran, N. N., Escriba-Gelonch, M., Saratraz, M. M., Pho, Q. H., Sagadevan, S., Hessel, V. (2023). Process Technology and Sustainability Assessment of Wastewater treatment. *Ind. Eng. Chem. Res.*, 62, 1195-1214. doi: 10.1021/acs.iecr.2c03471

United Nations. (2021, May). Report. Chapter 3: Renewable energy. Retrieved from https://sdgs.un.org/sites/default/files/2021-05/Report%20-%20Chapter%203%20-%20Renewable%20Energy.pdf

United Nations. (2023, November). Department of Economic and Social Affairs: Sustainable Development. Retrieved from https://sdgs.un.org/#goal_section

Vashisht, P. D., Ibhadon, A. O., Mehta, S. K., Taylor, M. J. (2024). Enhanced Wastewater Remediation Using Mesoporous Activated Wheat Straw Biochars: A Dye Removal Perspective. *ACS Sustainable Resource Management*, 1 (2), 355-367. doi: 10.1021/acssusresmgt.3c00109

Wang, Y., Lu, Y. (2023). Sodium Alginate-Based Functional Materials toward Sustainable Applications: Water Treatment and Energy Storage. *Ind. Eng. Chem. Res.*, 62, 11279-11304. doi: 10.1021/acs.iecr.3c01082

Weidner, E., Karbassiyazdi, E., Altaee, A., Jesionowski, T., Ciesielczyk, F. (2022). Hybrid Metal Oxide/Biochar Materials for Wastewater Treatment Technology: A review. *ACS Omega*, 7 (31), 27062-27078. doi: 10.1021/acsomega.2c02909

Yan, J., Oyedeji, O., Leal, J. H., Donohoe, B. S., Semelsberger, T. A., Li, C., Hoover, A. N., Webb, E., Bose, E. A., Zeng, Y., Williams, C. L., Schaller, K. D., Sun, N., Ray, A. E., Tanjore, D. (2020). Characterising Variability in Lignocellulosic Biomass: A Review. *ACS Sustainable Chem. Eng.*, 8, 8059-8085. doi: 10.1021/acssuschemeng.9b06263

Yin, Q., Nie, Y., Han, Y., Wang, R., Zhao, Z. (2022). Properties and the Application of Sludge-Based Biochar in the Removal of Phosphate and Methylene Blue from Water: Effects of Acid Treating. *Langmuir*, 38, 1833-1844. doi: 10.1021/acs.langmuir.1c02946

ZEISS. (2023, November). Research Microscopy Solutions: Sigma. Retrieved from https://www.zeiss.com/microscopy/en/products/sem-fib-sem/sem/sigma.html

Zeghioud, H., Fryda, L., Mahieu, A., Visser, R., Kane, A. (2022). Potential of Flax Shives and Beech Wood-Derived Biochar in Methylene Blue and Carbamazepine Removal from Aqueous Solutions. *Materials*, 15, 2824. doi: 10.3390/ma15082824

Zhang, B., Biswal, B. K., Zhang, J., Balasubramanian, R. (2023). Hydrothermal Treatment of Biomass Feedstocks for Sustainable Production of Chemicals, Fuels, and Materials: Progress and Perspectives. *Chem. Rev.*, 123, 7193-7294. doi: 10.1021/acs.chemrev.2c00673

Zhang, J., Zhang, Y., Zhao, W., Li, Z., Zang, L. (2021). Facile Fabrication of Calcium-Doped Carbon for Efficient Phosphorus Adsorption. *ACS Omega*, 6, 327-339. doi: 10.1021/acsomega.0c04642

Zheng, Y., Lv, P., Yang, J., Xu, G. (2023). Characterisation and Adsorption Capacity of Modified Biochar for Sulfamethylimidine and Methylene Blue in Water. *ACS Omega*, 8, 29966-29978. doi: 10.1021/acsomega.3c01251

911 Metallurgist. (2023, November). Particle Size Distribution: Types of Sieves. Retrieved from https://www.911metallurgist.com/particle-size-distribution/